공학박사학위논문

Unconstrained Monitoring of Sleep-Related Breathing Disorders and Sleep Stages Using A Polyvinylidene Fluoride Film Sensor

PVDF 필름 센서를 사용한 수면관련 호흡장애 및 수면 단계의 무구속적 모니터링

2015년 8월

서울대학교 대학원
협동과정 바이오엔지니어링 전공
황 수 환

Unconstrained Monitoring of Sleep-Related Breathing Disorders and Sleep Stages Using A Polyvinylidene Fluoride Film Sensor

PVDF 필름 센서를 사용한 수면관련 호흡장애 및 수면 단계의 무구속적 모니터링

지도교수 박 광 석

이 논문을 공학박사 학위논문으로 제출함

2015년 6월

서울대학교 대학원
협동과정 바이오엔지니어링 전공
황 수 환

황수환의 박사학위논문을 인준함

2015년 8월

위 원 장	김 희 찬	(인)
부위원장	박 광 석	(인)
위 원	정 도 언	(인)
위 원	이 유 진	(인)
위 원	박 철 수	(인)

Ph. D. Dissertation

Unconstrained Monitoring of Sleep-Related Breathing Disorders and Sleep Stages Using A Polyvinylidene Fluoride Film Sensor

Su Hwan Hwang

August 2015

Interdisciplinary Program in Bioengineering
The Graduate School
Seoul National University

Unconstrained Monitoring of Sleep-Related Breathing Disorders and Sleep Stages Using A Polyvinylidene Fluoride Film Sensor

BY
Su Hwan Hwang

Interdisciplinary Program in Bioengineering
The Graduate School
Seoul National University

THIS DISSERTATION IS APPROVED FOR THE DEGREE OF DOCTOR OF PHILOSOPHY

AUGUST 2015

Chairman	***Kim, Hee Chan, Ph.D.***
Vice Chairman	***Park, Kwang Suk, Ph.D.***
Member	***Jeong, Do-Un, M.D., Ph.D.***
Member	***Lee, Yu Jin, M.D., Ph.D.***
Member	***Park, Cheol Soo, Ph.D.***

ABSTRACT

Unconstrained Monitoring of Sleep-Related Breathing Disorders and Sleep Stages Using A Polyvinylidene Fluoride Film Sensor

Su Hwan Hwang

The Interdisciplinary Program in Bioengineering

The Graduate School

Seoul National University

In this study, unconstrained sleep-related breathing disorders (SRBD) and sleep stages monitoring methods using a polyvinylidene fluoride (PVDF) film sensor were established and tested. Subjects' physiological signals were measured in an unconstrained manner using the PVDF sensor during polysomnography (PSG). The sensor was comprised of a 4×1 array, and the total thickness of the system was approximately 1.1 mm. It was designed to be placed under the subjects' back and installed between a bed cover and mattress.

In the sleep apnea detection study, twenty six sleep apnea patients and six normal subjects participated. The sleep apnea detection method was based on the standard deviation of the PVDF signals, and the method's performance was assessed by

comparing the results with a sleep physician's manual scoring. The correlation coefficient for the apnea-hypopnea index (AHI) values between the methods was 0.94 ($p < 0.001$). For minute-by-minute sleep apnea detection, the method classified sleep apnea with average sensitivity of 72.9%, specificity of 90.6%, accuracy of 85.5%, and kappa statistic of 0.60.

In the snoring detection study, twenty patients with obstructive sleep apnea (OSA) participated. The power ratio and peak frequency from the short-time Fourier transform were used to extract spectral features from the PVDF data. A support vector machine (SVM) was applied to the spectral features to classify the data into either snore or non-snore class. The performance of the method was assessed using manual labelling by three human observers. For event-by-event snoring detection, PVDF data that contained "snoring" (SN), "snoring with movement" (SM), and "normal breathing" (NB) epochs were selected for each subject. The results showed that the overall sensitivity and the positive predictive values were 94.6% and 97.5%, respectively, and there was no significant difference between the SN and SM results.

In the sleep stages detection study, eleven normal subjects and thirteen OSA patients participated. Rapid eye movement (REM) sleep was estimated based on the average rate and variability of the respiratory signal. Wakefulness was detected based on the body movement signal. Variability of the respiratory rate was chosen as an indicator for slow wave sleep (SWS) detection. The performance of the method was assessed by comparing the results with manual scoring by a sleep physician. In

an epoch-by-epoch analysis, the method classified the sleep stages with average accuracy of 71.3% and kappa statistic of 0.48.

The experimental results demonstrated that the performances of the proposed sleep stages and SRBD detection methods were comparable to those of ambulatory devices and the results of constrained sensor based studies. The developed system and methods could be applied to a sleep monitoring system in a residential or ambulatory environment.

Keywords : Unconstrained Monitoring, Sleep Apnea, Snoring, Sleep Stages, PVDF Sensor

Student Number : 2009-23196

CONTENTS

LIST OF TABLES

LIST OF FIGURES

LIST OF ABBREVIATIONS

AASM	American Academy of Sleep Medicine
AHI	Apnea-hypopnea index
ANOVA	One-way analysis of variance
BCG	Ballistocardiogram
ECG	Electrocardiogram
EDR	ECG-derived respiration
EEG	Electroencephalogram
EMFIT	Electromechanical film
EMG	Electromyogram
EOG	Electrooculogram
FFT	Fast Fourier transform
HMMs	Hidden Markov models
HRV	Heart rate variability
IRB	Institutional Review Board
LOOCV	Leave-one-out cross validation
NB	Normal breathing
NW	NightWatch
OSA	Obstructive sleep apnea
PAT	Peripheral arterial tone
PCA	Principal component analysis

PF	Peak frequency
PPV	Positive predictive value
PR	Power ratio
PSG	Polysomnography
PVDF	Polyvinylidene fluoride
REM	Rapid eye movement
RERAs	Respiratory event-related arousals
ROC	Receiver operating characteristics curve
SaO2	Blood oxygen saturation
SM	Snoring with movement
SN	Snoring
SNR	Signal-to-noise ratio
SNUH	Seoul National University Hospital
SpO2	Oxygen desaturation
SRBD	Sleep-related breathing disorder
STFT	Short-time Fourier transform
SVM	Support vector machine
SWS	Slow wave sleep

CHAPTER 1. INTRODUCTION

1.1. Background

Sleep affects our physical and mental health and our daily functioning in many ways. Many previous studies have reported that sleep is associated with increased waste clearance in the brain [1], restoration [2, 3], ontogenesis [4-6], memory processing [7-10], preservation of memory [11, 12], etc. Because sleep plays a vital role in our lives, chronic sleep deprivation can lead to elevated mortality risk [13], increased risk of coronary events [14], obesity [15], and diabetes [16]. Other studies have found that sleep loss is related to metabolism [17, 18], immunity [19-21], and cardiovascular issues [13, 22, 23]. Thus, continuous sleep monitoring is very important to maintain a healthy life.

Polysomnography (PSG) has been regarded as the standard method for general sleep monitoring. PSG results include sleep duration, sleep stages, sleep-related disorders, sleep fragmentation, and sleep quality. Even though PSG has been used for the assessment of sleep, monitoring sleep and sleep-related disorders using PSG has a few limitations. Firstly, PSG recording during sleep is an inconvenient experience for the sleeper because numerous sensors are attached to the sleeper's body and face, as shown in Figure 1-1. Secondly, PSG recording requires well-trained sleep experts, a controlled hospital environment, and a relatively long setup time, which results in high costs. Lastly, the manual scoring of sleep stages and

sleep-related events from PSG data is a very time consuming and laborious process. The drawbacks of sleep monitoring based on PSG recording limit its use in a specialized sleep laboratory. If sleep and associated events can be monitored based on an automated algorithm without attaching any sensors to the sleeper's body, the convenience of sleep monitoring will be greatly increased, and make it suitable for residential or ambulatory monitoring purposes.

Figure 1-1. Sensors for polysomnography.

1.2. Sleep Apnea

Sleep apnea is a typical sleep related-breathing disorder (SRBD) characterized by frequent, abnormal cessation of respiration during sleep [24]. During the apneic period, there is an increased effort in breathing, leading to arousal and sleep fragmentation [25]. Thus, severe and frequent sleep apnea disrupts the sleep architecture of subjects and can lead to sleep disorders such as severe snoring [26], fatigue, daytime sleepiness [27], and systemic hypertension [28]. In addition, apnea-induced hypoxia during sleep can cause stroke [29], arrhythmias [30], diabetes [31], and cardiovascular diseases [32]. Figure 1-2 shows the mechanism of sleep apnea.

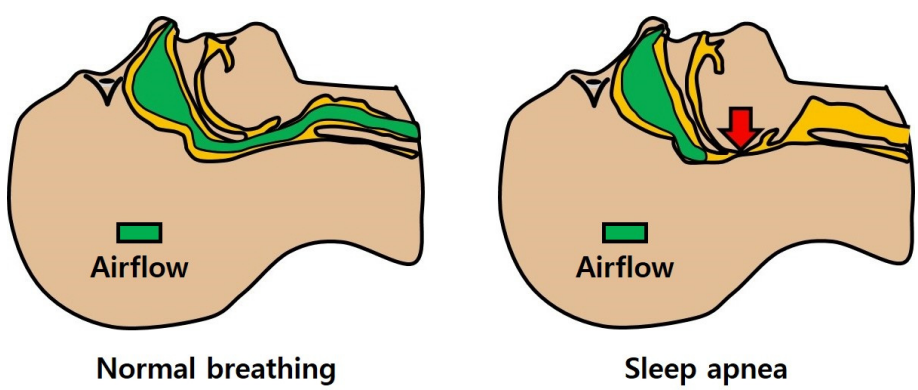

Figure 1-2. The mechanism of sleep apnea.

In previous study, Young *et al.* reported that approximately 2% of adult women and 4% of adult men in the middle age range are affected by sleep apnea [33]. Kim *et al.* analyzed data to determine the prevalence of SRBD in 457 Korean adults aged 40–69 years and 27% of men and 16% of women, respectively, had SRBD [34]. Furthermore, a recent study of SRBD in adults discovered the actual prevalence rates of SRBD representing substantial increase over the last two decades (10% among 30–49-year-old men; 17% among 50-70-year-old men; 3% among 30-49-year-old women; and 9% among 50-70-yearold) [35].

In recent years, many alternative methods without using PSG to detect apneic or hypopnic events have been proposed. These studies have involved sleep apnea detection based on several biosignals. For example, electrocardiogram (ECG) based studies have shown that RR interval or R peak amplitude based methods are useful for apnea detection [36-39]. A ballistocardiogram (BCG) based system measured the respiratory rate with high correlation using an air mattress with a balancing tube [40]. Pulse oximetry and respiratory signal based studies revealed a relatively high correlation coefficient ($r > 0.9$) between the apnea-hypopnea index (AHI) from PSG and the proposed one [41, 42]. Despite these efforts, a clearly superior method or system for fully unconstrained sleep apnea monitoring still does not exist.

1.3. Snoring

Snoring is one of the SRBD characterized by loud, noisy respiratory sounds during sleep, caused by the vibration of the soft palate and the uvula [43]. The mechanism of snoring is shown in Figure 1-3. Snoring is common in the general population, and the prevalence of snoring varies widely among studies: 24-86% of men and 14-57% of women [44-47]. Some previous studies have shown that snoring is associated with excessive daytime sleepiness [48], and hypertension [49, 50]; however, it is difficult to ascertain how many of these health risks are attributable to snoring alone [51].

Nonetheless, snoring detection has clinical significance because snoring may indicate undiagnosed obstructive sleep apnea (OSA) [52]. Apnea-induced hypoxia during sleep can also lead to severe cardiovascular disease [32, 53]. Additionally, severe and frequent snoring can disrupt the spouse's sleep [45].

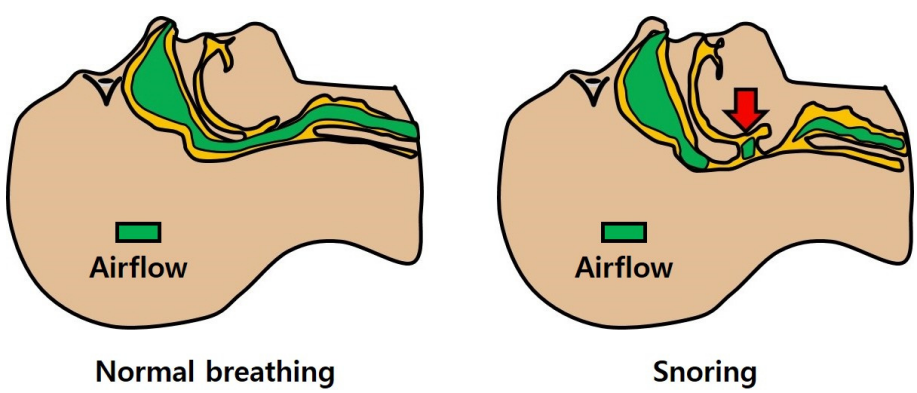

Figure 1-3. The mechanism of snoring.

According to the manual issued by the American Academy of Sleep Medicine (AASM) for scoring sleep and associated events, an acoustic sensor (such as a microphone), piezoelectric sensor, or nasal pressure transducer are recommended for snoring monitoring during PSG [54]. Although PSG has been used for the assessment of SRBD, some PSG reports do not provide objective information about snoring (number of occurrences, duration, etc.) because snoring recording during PSG is optional [54] and is used to assess only the existence of snores rather than the details of snoring occurrences.

To overcome these limitations, other previous studies have proposed acoustic snoring evaluation methods without PSG. Most of these methods implement one or more microphones placed on the trachea or a location close to the sleeper's bed (freestanding, near the mouth, or over the head) [55-59]. Although snoring events were detected successfully by these methods (sensitivity ranging from 82.2% to 94.8%), these microphone-based methods can be affected by ambient noise and their performance can vary depending on the position of the microphone [60]. Furthermore, microphone-based methods require a high sampling rate of over 10 kHz to analyze the acoustic characteristics of the snoring sounds, and the high processing cost of the necessary microcontroller may render these methods unsuitable for residential or ambulatory monitoring devices.

Alternative snoring detection methods without using microphones have also been investigated. Shin *et al.* evaluated the performance of noninvasively monitoring the events of snoring using an air mattress with a balancing tube system [61]. Although

the system unconstrainedly measured a subject's snoring signals, a detection process was not applied on data acquired during real nocturnal sleep. Lee *et al.* proposed a snoring detection method based on a piezoelectric snoring sensor that measured the vibration related to snoring [62]. However, this piezoelectric snoring sensor was attached to the neck during PSG recording, and the attachment of the sensor could interrupt comfortable sleep. In brief, these alternative attempts did not provide a fully unconstrained snoring detection method.

1.4. Sleep Stages

The AASM manual for sleep scoring [54] divides it into five stages: wake, rapid eye movement (REM), and N1–N3 (non-REM 1, 2, and 3). Stage N3 is also called delta sleep or slow wave sleep (SWS) [63]. These stages progress in a cycle from stage N1 to REM, and then the cycle starts over again with stage N1. A normal young adult spends almost 50% of their total sleep time in stage N2, about 20% in stage REM, and the remaining 30% in the other stages [51]. Non-REM (NREM) sleep and REM sleep alternate, usually with four or five periods of approximately 90 min per night [64]. Figure 1-4 shows a typical example of a normal adult's hypnogram.

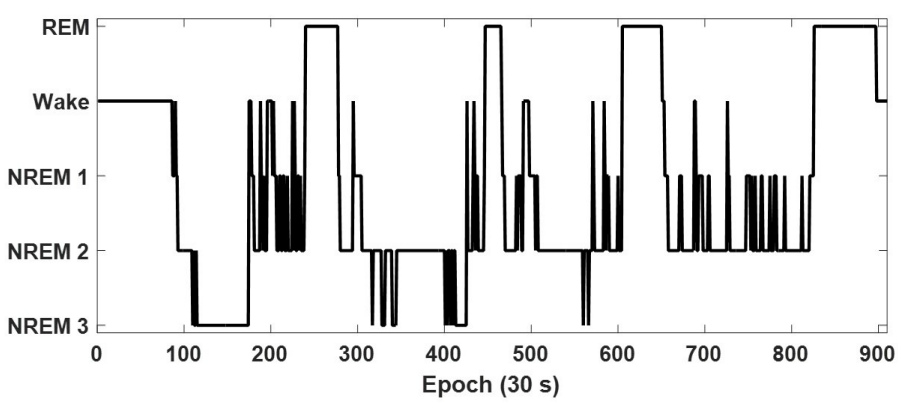

Figure 1-4. A hypnogram of normal adult.

The sleep stages can be determined by an electroencephalogram (EEG), electrooculogram (EOG), and chin electromyogram (EMG). In order to measure these types of physiological signals during sleep, numerous sensors or electrodes are attached to the head, face, and body of the sleeper. However, the attachment of numerous types of sensors can interrupt comfortable sleep, which makes daily sleep monitoring difficult using EEG-based methods.

To overcome these limitations, sleep stages detection methods using a minimum of sensors have been proposed in previous studies. Most of these methods implement heart rate variability (HRV) or ECG-derived respiration (EDR) features from an ECG signal to classify the sleep stages [65-68]. Another example is a method based on peripheral arterial tone (PAT) signal [69]. Although the sleep stages could be detected using these methods (with accuracies ranging from 56.0% to 72.6%), the attachment of the sensor to measure the physiological signal during sleep can still cause a great deal of inconvenience to the sleeper.

Alternative sleep stages detection methods without any attachment of a sensor to the sleeper's body have also been proposed. Watanabe *et al.* used a pneumatic bio measurement sensor to estimate the sleep stages thorough unrestrained means [70]. Although they showed the potential for unconstrained sleep monitoring, their overall epoch-by-epoch accuracy was only 42.8%. Kortelaine *et al.* evaluated the sleep structure using an electromechanical film (EMFIT) sensor [71]. They used a BCG and the movement activity obtained from a sensor to detect the sleep stages. Samy *et al.* described an unobtrusive method for sleep stages detection based on a pressure

sensitive bed sheet [72]. The respiration and leg movement signals were selected as features for sleep stages identification in that study. Although previous studies have proposed unconstrained sleep stages detection methods, all of these methods classified sleep into only three stages (wake, REM, and NREM; the macrostructure of sleep), which do not provide sufficient data for a microstructure analysis of sleep. Therefore, an unconstrained sleep stages monitoring method that provides data for at least a four stage analysis is required.

1.5. Polyvinylidene Fluoride Film Sensor

Polyvinylidene fluoride (PVDF) film is a very thin and flexible film that is widely used in film transducer or speaker elements [73]. This piezoelectric polymer is good for applications where mechanical loads are applied [74]. In particular, it can be applied where signal-to-noise requirements influence very low mass loading by the sensors.

In previous studies, a PVDF film was used as a sensor for recording several bio signals such as the respiration [75-77], heart rate [78], and BCG [79, 80]. Furthermore, PVDF based SRBD events or sleep stages detection methods have also been proposed in the literature. Berry *et al.* compared the capability of a PVDF thermal sensor attached to the upper lip with a pneumotachograph to detect respiratory events in OSA patients [81]. Koo *et al.* used PVDF incorporated belts surrounding the chest and abdomen to validate respiratory event classification during PSG [82]. Norman *et al.* evaluated a PVDF based contactless monitoring system (Sonomat) for the diagnosis of SRBD [83].

Although these studies constrainedly or unconstrainedly measured a subject's physiological signals to evaluate SRBD events, to the best of my knowledge, fully unconstrained systems or methods for monitoring SRBD events with the sleep stages using signals measured by PVDF sensors have rarely been studied.

1.6. Purpose

As mentioned in the previous sections, there is a need for a sleep monitoring system and analytical methods to simultaneously analyze both the sleep stages and SRBD events. Furthermore, physiological signal measurement during sleep without the sleeper consciously feeling the presence of the installed sensor is essential for long-term residential sleep monitoring purposes.

Therefore, this study was conducted to establish a fully unconstrained sleep monitoring method using a PVDF sensor for the continuous and accurate monitoring of both the sleep stages and SRBD events.

This study had the following three goals:

1) The development of a sleep apnea monitoring method with highest level of performance, comparable to that of a commercial device;
2) The development of a snoring monitoring method with low computational cost and robustness with regard to motion artifacts;
3) The development of a sleep monitoring method that can classify sleep into four stages in an unconstrained manner.

CHAPTER 2. SLEEP APNEA DETECTION

2.1. Signal Acquisition System

The physiological signals of the subjects during sleep were measured using the PVDF film sensor. The sensor was composed of a 4 × 1 array positioned under the subject's back. It was installed between a mattress cover and the mattress to avoid direct contact with the subject's body. The shape and size of the sensor, and a conceptual diagram of the system installation, are shown in Figure 2-1 [84].

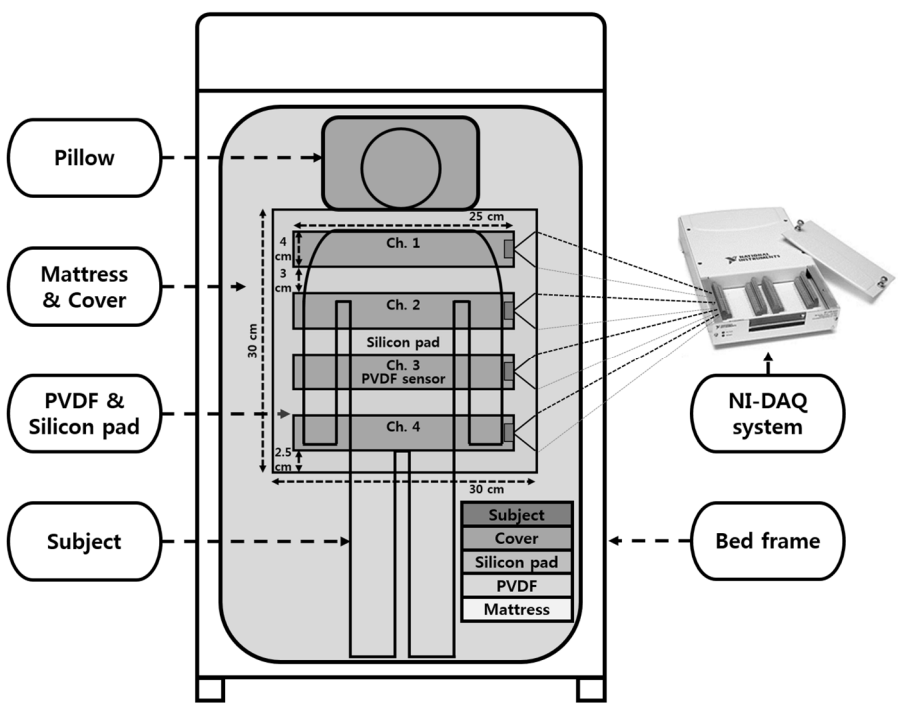

Figure 2-1. Conceptual diagram of system size and installation.

The total thickness of the sensor and its protective silicon pad was 1.1 mm, which was sufficiently thin to prevent the subject from being consciously aware of its presence. The sensor was a 122μm thick silver ink metalized piezoelectric film sensor (part number: 3-1004-346-0, Measurement Specialties, Inc., Hampton, VA, USA). Its specifications are shown in Table 2-1.

Table 2-1. Typical specifications of a commercialized PVDF film.

Electro-Mechanical Conversion	(1 direction) 23 x 10^{-12}m/V, 700 x 10^{-6}N/V
Mechano-Electrical Conversion	(1 direction) 12 x 10^{-3}V per microstrain,
	400 x 10^{-3}V/μm, 14.4V/N
Capacitance	1.36 x 10^{-9}F; Dissipation Factor of 0.018 @ 10 KHz;
	Impedance of 12 KΩ @ 10 KHz
Maximum Operating Voltage	DC : 280 V (yields 7 μm displacement in 1 direction)
	AC : 840 V (yields 21 μm displacement in 1 direction)
Maximum Applied Force	6−9kgF (yields voltage output of 830 to 1275 V)

PVDF data were collected from July 2012 to October 2013, and the sensor's durability over more than one year was verified. During the experiments, sweat did not affect signal quality because the PVDF sensor's functionality is mainly based on its piezoelectric properties. After PSG recording, none of the subjects reported an uncomfortable feeling, and all responded that the sensor did not interfere with their sleep. Because the subjects did not experience physical or mental stress, it can be concluded that the proposed sensor is appropriate for unconstrained sleep monitoring.

The Institutional Review Board (IRB) of Seoul National University Hospital (SNUH) approved all of these procedures. All of the participants were provided with information about the methods and purpose of the study and informed consent approved by the IRB was obtained.

2.2. Methods

2.2.1. Participants and PSG Data

Thirty-two subjects participated in this study. Twenty-eight nocturnal PSG datasets were collected at the SNUH Center for Sleep and Chronobiology. Four diurnal PSG datasets were additionally recorded for the relatively young (<30 years) participants. All of the PSG datasets were collected based on the standard PSG routine and scored by registered PSG technologist who has more than ten years' experience in scoring human sleep records according to the criteria of AASM [54]. Additionally, scoring result were reviewed and confirmed once again by a trained sleep physician. Using the international 10–20 system, EEG electrodes were placed at the O2-A1 and C3-A2 positions. In addition to the EEG data, bilateral EOG, EMG from the chin and bilateral tibialis anterior muscles, lead II ECG, oronasal airflow, abdominal and thoracic movement, snoring, and oxygen desaturation (SpO2) signals were also collected. During sleep, the subject's respiratory signals from the PVDF film sensor were simultaneously recorded with the PSG data. All of the signals were measured using an NI-DAQ 6221 (National Instruments, Austin, TX, USA) data acquisition unit with a 250 Hz sampling rate. A summary of the subject and PSG-related parameters is presented in Table 2-2.

Table 2-2. Sleep related parameters of subjects for sleep apnea detection.

AHI (events/hour)	Normal <5	Mild 5-15	Moderate 15-30	Severe >30
Average AHI	3.3±0.8	10.4±2.3	22.4±3.4	41.2±7.9
PSG (N/D)	5 (4/1)	10 (7/3)	7 (7/0)	10 (10/0)
Gender (M/F)	4/1	10/0	5/2	9/1
Age (years)	38.4±20.7	36.1±15.7	56.3±17.0	56.7±9.3
BMI (kg/m^2)	22.2±1.9	23.9±2.3	24.9±1.2	28.7±3.1
Total sleep time (min)	372.9±149.7	291.7±144.5	437.5±21.0	410.3±40.8
Total wake time (min)	37.2±36.3	26.1±20.8	14.0±8.6	14.5±6.5
Sleep efficiency (%)	84.1±5.8	78.5±11.6	89.2±5.3	85.4±6.6
Sleep latency (min)	13.6±12.1	20.7±29.1	7.3±5.1	5.2±3.7
% stage 1 NREM	10.3±5.9	14.4±4.1	17.8±5.3	28.8±8.8
% stage 2 NREM	48.6±9.1	45.8±10.2	52.5±9.1	37.9±8.9
% stage 3 NREM	11.3±8.7	8.2±7.2	4.0±3.2	0.9±1.1
% stage REM	17.9±3.4	16.0±6.9	15.9±4.0	18.8±5.9
Ave. SpO2 (%)	97.4±1.2	96.7±1.6	96.2±1.6	94.8±1.6
Min. SpO2 (%)	91.7±2.7	89.9±4.0	84.8±7.2	79.1±7.1

AHI: apnea hypopnea index; BMI: body mass index; N: nocturnal;
D: diurnal; NREM: non-rapid eye movement sleep;
REM: rapid eye movement sleep; Ave.: average; Min.: minimum;
SpO2: oxygen saturation

2.2.2. Apneic Events Detection

The study about an unconstrained sleep apnea detection was published as a journal paper [85]. During the inhalation and exhalation respiratory phases, different levels of pressure caused by the volume change in the body were applied to the PVDF sensor. As a result, the output signals of the sensor reflect the normal or apneic breathing of the subjects.

As shown in Figure 2-2, the signal outputs from the PVDF sensor included several types of physiological signals, including those for respiration, BCG, and body movement [85]. When an apneic event occurred, the change in the PVDF signal was relatively small compared with the other cases. Thus, to distinguish apneic events from normal breathing or body movement, the standard deviation of PVDF signals was used in this study. To determine a method for apnea monitoring, PSG and PVDF data from six subjects (approximately 20%) with normal to severe apnea were randomly selected as a training set. All of the detection procedures for apneic events are concisely described in Figure 2-3 [85]. All values used in the conditions in this figure were determined based on the training dataset. For example, Figure 2-4 shows value determination for the upper threshold of the apneic event decision.

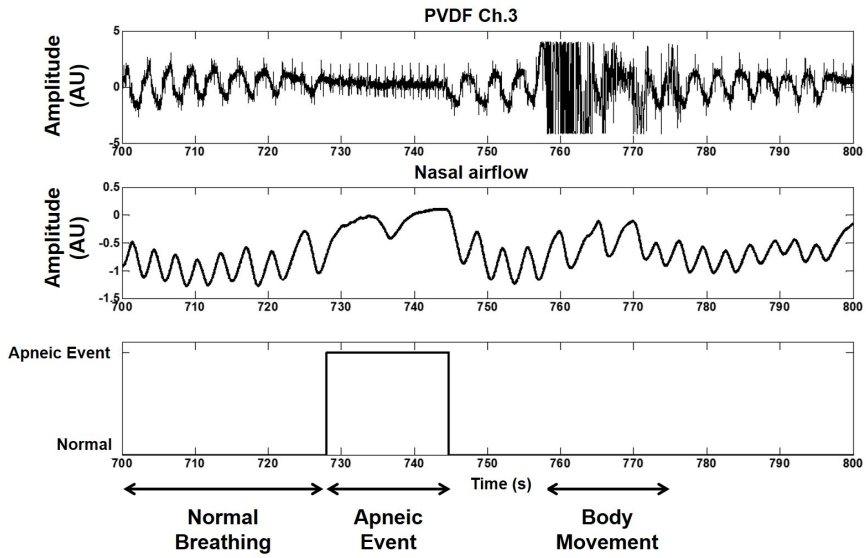

Figure 2-2. Signal output from the PVDF sensor for sleep apnea detection.

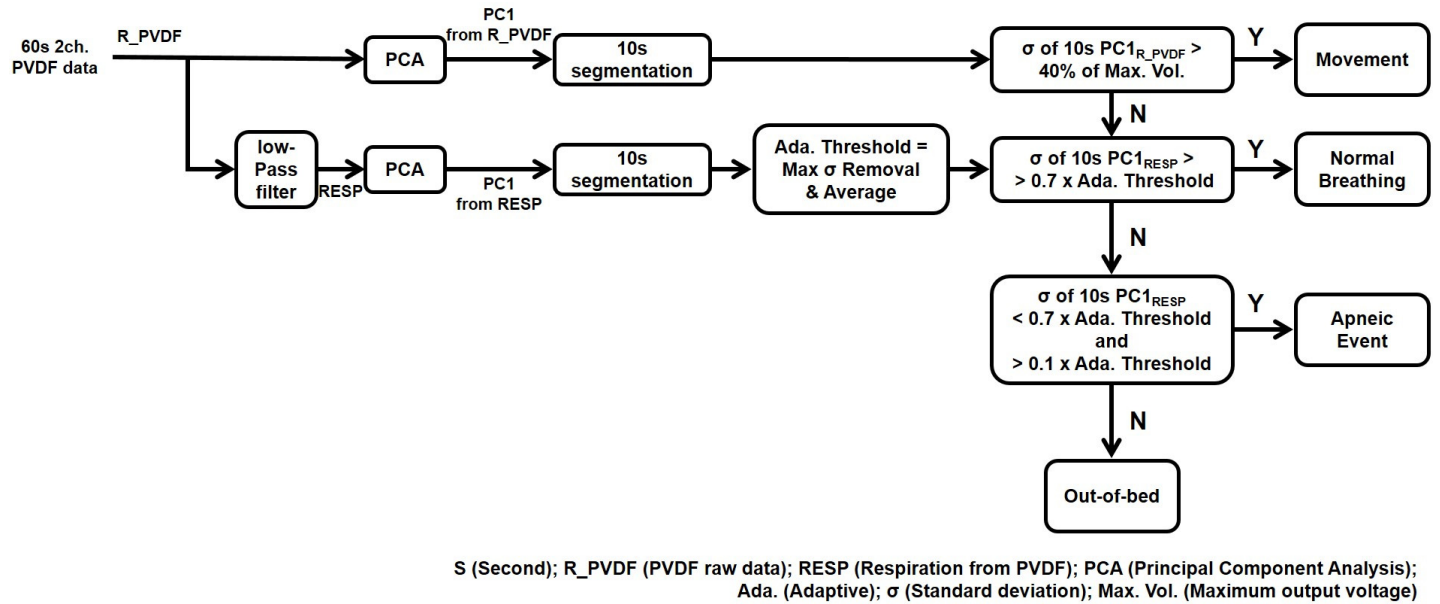

Figure 2-3. Apneic event detection procedure.

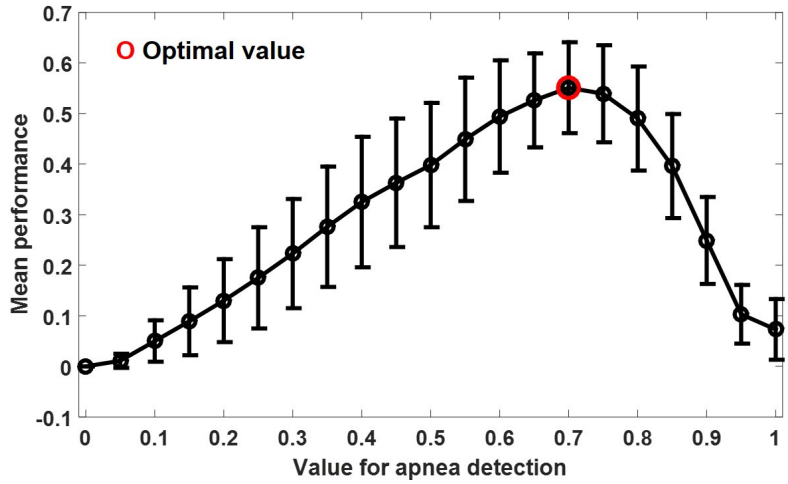

Figure 2-4. Value determination for threshold of sleep apnea detection.

From the analysis of the training set, the data from PVDF channels #3 and #4, which reflected changes in the abdomen volume induced by breathing, were selected for the final analysis. At 60 s intervals, the raw signal (R_PVDF) data from each PVDF channel were low-pass filtered at 0.5 Hz (5^{th} order, IIR Butterworth) and both channel respiratory signals (RESP) were obtained. After that, principal component analysis (PCA) was applied to R_PVDF and RESP, respectively. PCA is a well-known method for feature extraction and is defined as an orthogonal linear transformation. PCA reduces the dimensionality of a data matrix to find new variables using the eigenvectors with the largest eigenvalues. These are sorted according to decreasing eigenvalue, and the eigenvalues with lower significance are discarded. In this way, the data dimensionality is decreased with a minimal loss of information [86]. Thus, to obtain a common feature between the two channels' data and to reduce the noise contamination, PCA factor 1 (PC1) was extracted from the R_PVDF ($PC1_{R\_PVDF}$) and RESP ($PC1_{RESP}$).

After applying PCA, 60 s data sets from $PC1_{R\_PVDF}$ and $PC1_{RESP}$ were divided into 6 periods of 10 s each. Before the threshold determination, the standard deviation of each 10 s data set from $PC1_{RESP}$ was calculated. In the following (2-1), x_m and x_k denote a 10 s $PC1_{RESP}$ data set and 10 s $PC1_{R\_PVDF}$ data set, and σ_m and σ_k represent the standard deviations of x_m and x_k, where m and k are segment numbers ($1 \leq m, k \leq 6$).

$$\boldsymbol{\sigma_m = \sqrt{E(x_m^2) - (E(x_m))^2}}, \quad \boldsymbol{\sigma_k = \sqrt{E(x_k^2) - (E(x_k))^2}} \qquad \textbf{(2-1)}$$

To minimize the underestimation of apnea because of an increased threshold caused by body movement, the threshold was selected using the average of the remaining values, with the exception of the largest value, among σ_m. In this way, an adaptive threshold for $PC1_{RESP}$ for every 60 s period could be obtained.

$$\textbf{Adaptive threshold} = \frac{1}{5}\sum_{m=1, m\neq j}^{6} \sigma_m, \qquad \textbf{(2-2)}$$

$$\textbf{where } \sigma_j = \max\{\sigma_m\}, 1 \leq m \leq 6$$

Using σ_k and σ_m, each body movement, normal breathing, apneic event, or out of bed period was determined based on the following conditions, which are listed according to their priority. In this study, the maximum output voltage of the PVDF signals was 5 V.

Condition 1: (for movement)

$\sigma_k > 0.4 \times$ maximum output voltage

Condition 2: (for normal breathing)

$\sigma_m > 0.7 \times$ adaptive threshold

Condition 3: (for apneic event)

$0.1 \times$ adaptive threshold $< \sigma_m < 0.7 \times$ adaptive threshold

Condition 4: (for out of bed event)

$\sigma_m < 0.1 \times$ adaptive threshold

All the values used for the conditions were based on the training dataset. For instance, the upper threshold was determined by the mean performance evaluation of the training set for an apneic event decision. As shown in Figure 2-4, when the value for the upper threshold of an apneic event decision was 0.7, the mean performance was the highest. Interestingly, this 70% threshold level for an apneic event decision corresponded to standard hypopnea scoring rules [54]. In this analysis, Cohen's kappa (k) coefficient was marked as the "mean performance." All the analyses were performed using MATLAB software (MathWorks Inc., USA, R2015a version).

2.2.3. Statistical Analysis

To evaluate the AHI estimation performance, a linear regression analysis was used for the correlation coefficient, and the Bland-Altman method was used to assess the agreement [87]. In this analysis, statistical significance at the 5% level was used. In addition, the sleep apnea diagnosis was conducted based on three levels of AHI cut-off values because there was no threshold value for AHI that clearly discriminated patients with and without sleep apnea [41].

According to the minute-by-minute analysis, if apneic events occurred more than once (up to 6), the current minute was considered to be an "estimated apnea minute ($Apnea_{EST}$)." The same rule was applied to the apneic events from PSG ($Apnea_{PSG}$), and minute-by-minute statistical analyses between $Apnea_{EST}$ and $Apnea_{PSG}$ were performed. The sensitivity, specificity, and accuracy were used for these statistical analyses.

In the analysis, the sensitivity denoted the proportion of correctly identified apnea minutes, while the specificity denoted the proportion of other correctly identified states. In addition, the performance of the proposed method was quantified using Cohen's kappa, which is very commonly used for studies that measure the agreement between two separate evaluators [88].

2.3. Results

2.3.1. AHI Estimation

To evaluate the performance of the system, the algorithm determined by the training dataset was applied to the test dataset, and the apneic event estimation results were compared with the ones from PSG. The AHI from the proposed method (AHI_{EST}) was compared with the one from PSG (AHI_{PSG}). As shown in Figure 2-5(a) [85], a significant correlation (Pearson's correlation coefficient = 0.94, $p < 0.001$) was found between AHI_{EST} and AHI_{PSG}. Figure 2-5(b) shows the agreement between AHI_{EST} and AHI_{PSG}, which was evaluated by using the Bland-Altman method. In this figure, the mean difference between the AHI values was 2.3 events/h (no significant difference) and approximately 96% (25 of 26) of the cases were within the dashed lines (95% confidential interval, from –15.0 to 10.2).

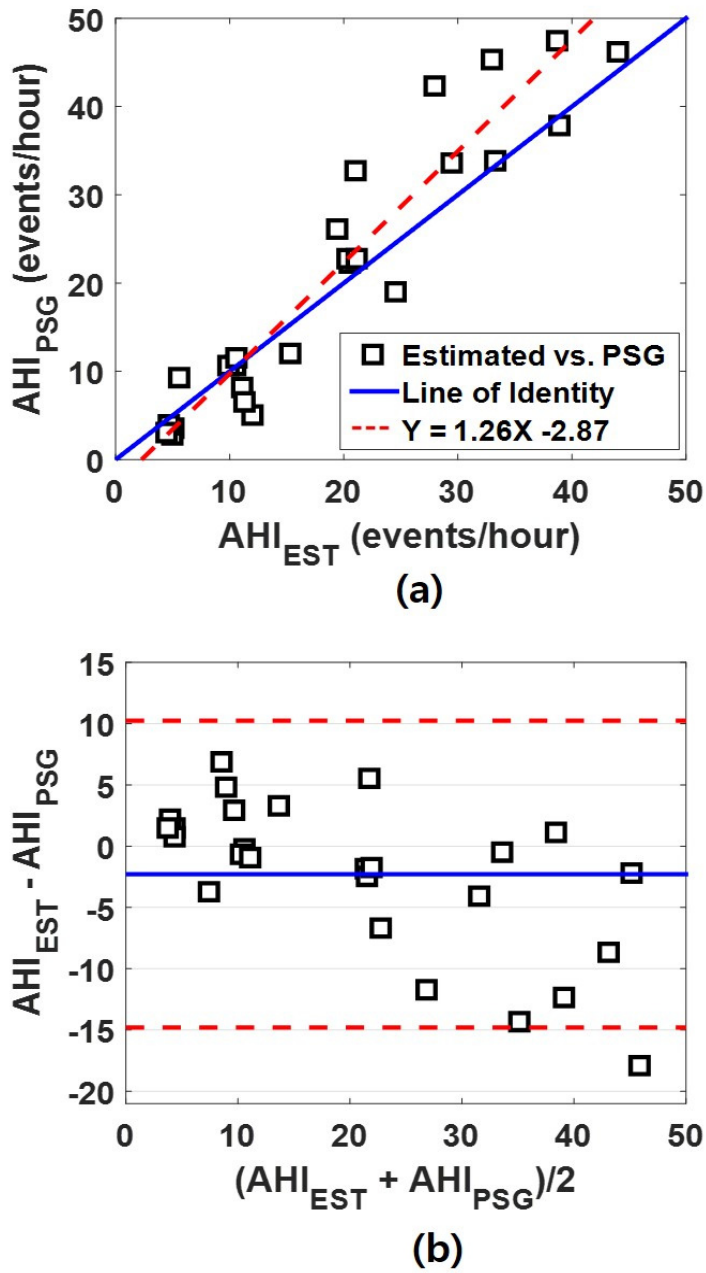

Figure 2-5. Relationship between AHIs from PSG and proposed method.

Table 2-3 shows a comparison between the AHI estimation results from the proposed method and those from previous methods. The results from the oronasal airflow based [42] and PVDF thermal sensor based methods [37] had similar performances compared with proposed ones. In other studies, a nasal airflow based method [89] showed a higher correlation coefficient than proposed method, while a peripheral arterial tonometry based method [41] showed a lower correlation coefficient than the one from proposed method. In Table 2-3, concordance means the ratio of cases that were within 2 standard deviations in the Bland-Altman plot.

Table 2-3. Comparisons of sleep apnea detection results with previous studies.

Author (year)	Method	N	R	*p*	Concordance
Han (2008)	Nasal Airflow	21	0.98	< 0.01	20/21
Ayas (2003)	Peripheral arterial tonometry, SaO2	30	0.87	< 0.001	26/30
White (1995)	Oronasal airflow, SaO2, chest & abdominal motion	30	0.94	< 0.001	n/a
Nakano (2007)	PVDF thermal sensor	299	0.94	< 0.001	n/a
Koo (2011)	PVDF impedance belts	50	0.91	n/a	n/a
Hwang (2015)	**PVDF sensor**	**26**	**0.94**	**< 0.001**	**25/26**

N: number of participants; R: Pearson's correlation coefficient; *p*: P-value

2.3.2. Diagnosing Sleep Apnea

With AHI thresholds of 5, 15, and 20 events per hour, the sleep apnea diagnosis results for the test dataset were assessed using various statistical values. As shown in Table 2-4, for all of the AHI thresholds, the kappa statistic revealed almost perfect agreement ($k > 0.8$), and the area under the receiver operating characteristics curve (ROC) was greater than 0.98. At AHI thresholds of 5 and 15, there was one false positive in each case. However, the estimated AHIs slightly exceeded each AHI cut-off level (5.1 and 15.3 events/hour).

Table 2-4. Diagnostic results at three AHI threshold levels.

Parameter	AHI > 5	AHI > 15	AHI > 20
Sensitivity (%)	100	100	92.3
Specificity (%)	75	91.7	92.3
PPV (%)	95.7	93.3	92.3
NPV (%)	100	100	92.3
Accuracy (%)	96.2	96.2	92.3
Kappa statistic	0.84	0.92	0.85
ROC AUC	0.98	0.99	0.98

AHI: apnea hypopnea index; PPV: positive predictive value;
NPV: negative predictive value;
ROC AUC: area under the receiver operating characteristics curve

2.3.3. Minute-By-Minute Sleep Apnea Detection

The minute-by-minute sleep apnea detection results are shown in Table 2-5. From the test dataset, each statistical result was calculated depending on the severity of AHI. From the normal (AHI < 5) to severe level (AHI > 30), the specificity and accuracy were gradually decreased. A kappa statistical analysis revealed a borderline case between substantial ($0.6 < k < 0.8$) and moderate agreement ($0.4 < k < 0.6$), whereby the overall $k = 0.6$ [90].

Table 2-5. Minute-by-minute sleep apnea detection.

Set	Group		N	Sensitivity (%)	Specificity (%)	Accuracy (%)	Kappa statistic
Training	Total		6	69.4±6.3	91.1±7.3	84.5±7.3	0.58±0.06
Test	Total		26	72.9±10.9	90.6±6.5	85.5±6.6	0.60±0.10
		Normal	4	72.7±9.6	96.9±1.0	95.4±1.2	0.63±0.07
	Apnea	Mild	8	68.8±15.6	92.4±3.1	88.4±3.2	0.57±0.12
	Severity	Moderate	5	74.1±7.0	88.7±4.8	82.9±2.2	0.63±0.04
		Severe	9	75.9±8.7	87.3±8.5	80.0±5.4	0.59±0.11

N: number of participants; AHI: apnea hypopnea index

Figure 2-6 shows apnea minute estimation results for the best case (Figure 2-6(a), subject #5) and worst case (Figure 2-6(b), subject #21) from the nocturnal data [85]. In the best case, AHI, sensitivity, specificity, accuracy, and kappa statistic were 46.2 events/h, 91.9%, 88.7%, 90.8%, and 0.79, respectively. In the worst case, the corresponding values were 5.1 events/h, 82.9%, 87.7%, 87.3%, and 0.45, respectively.

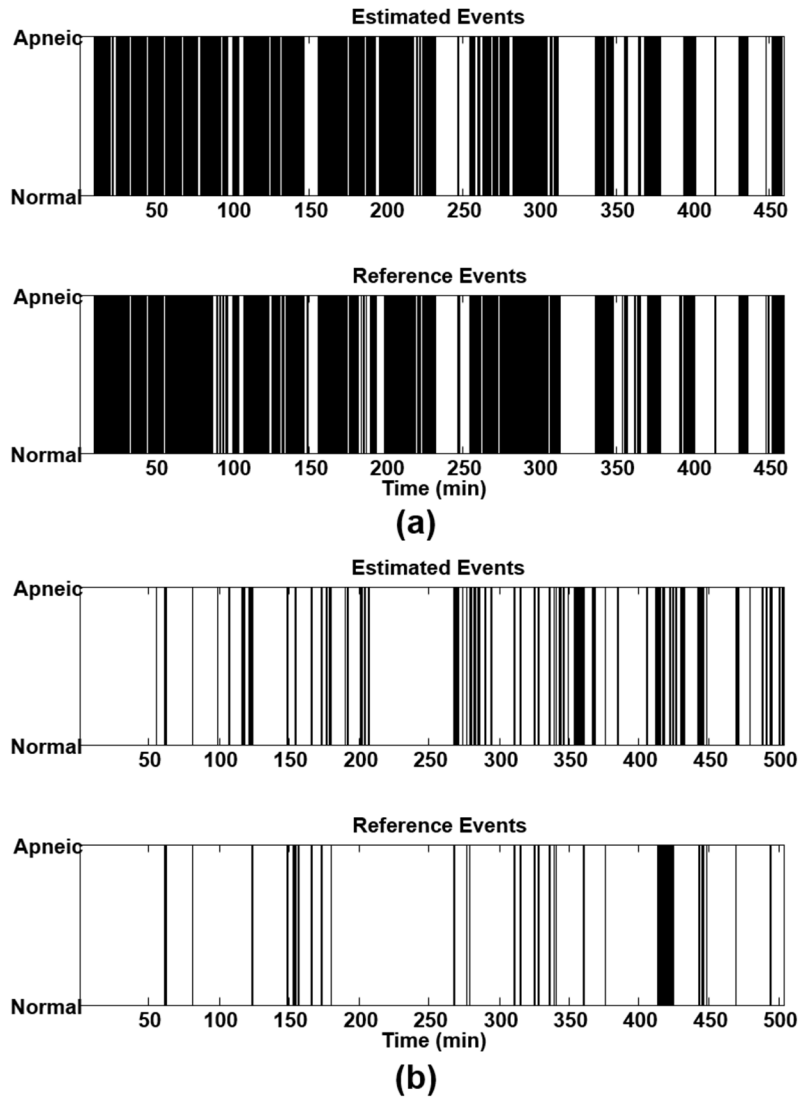

Figure 2-6. Minute-by-minute sleep apnea detection results for the best and worst cases.

2.4. Discussion

2.4.1. Agreement between Proposed Method and PSG

The apnea detection process was based on the following steps: 1) extraction of the respiratory signal from the PVDF data; 2) principal component extraction and data segmentation; 3) threshold determination; and 4) apneic event decisions. When the proposed method was applied to the test dataset, it was shown that the estimated AHI from the proposed method was significantly correlated with the one from PSG (Figure 2-5(a)). In the minute-by-minute analysis (Table 2-5), for all of the subjects, the kappa statistics revealed greater than moderate agreement ($k > 0.4$). Furthermore, about half (12 of 26) of the subjects showed substantial agreement ($k > 0.6$) in the test set. Other results (Table 2-4) showed that the proposed algorithm could accurately diagnose the sleep apnea patients based on the high accuracy and agreement of the results. Consequently, it can be concluded that the results of sleep apnea detection method were comparable to those of PSG. Because the PVDF film based method is simple and does not require trained experts, if combined with signal processing unit, it can be used for ambulatory sleep apnea monitoring. Moreover, it can support apnea event detection during PSG recording.

2.4.2. Comparisons with Previous Studies

The proposed sleep apnea detection method had an accuracy similar to that for the ambulatory device that is currently used in clinical practice or constrained PVDF based methods (Table 2-3). For instance, Ayas *et al*. used a wrist-worn device that

combines PAT, actigraph, and arterial oxygen saturation to diagnose OSA [41]. Even though the device used the attenuation of the PAT signal amplitude, which is strongly correlated with apnea [91], along with the blood oxygen saturation (SaO2) signal, which directly reflects the absence of breathing, the correlation coefficient between PSG AHI and the wrist-worn device was lower than that of the proposed one. Another example is the NightWatch (NW) system, which records the SaO2, oronasal airflow, and chest and abdominal wall motion using sensors attached to the patient's face and body [42]. White *et al*. assessed the accuracy of the NW system used at home and in the lab to monitor sleep apnea. Although NW collected many physiological signals for apnea detection, its AHI estimation performance was similar to results from this study. Han *et al*. also detected apneic events using a single nasal airflow channel from PSG data [89]. The performance of their method was found to be better than the proposed one in a linear regression analysis of AHI, while the concordance on the Bland-Altman plot calculated in this study was slightly higher than that found in their study.

Koo *et al*. detected respiratory events using PVDF impedance belts surrounding the patient's chest and abdomen [82], and their method was comparable to standard respiratory inductance plethysmography in determining respiratory events during PSG. Nakano *et al*. monitored oronasal airflow using a PVDF thermal sensor, and found that an airflow monitor could be used to detect sleep-disordered breathing [37]. Berry *et al*. compared the readings from a PVDF thermal sensor attached to the upper lip with a mask pneumotachograph and accurately detected respiratory events

compared with the detection accuracy of pneumotachograph in patients with OSA [81]. Even though they used belts or a thermal sensor that could directly measure the respiratory-induced signals, there were no significant differences in the AHI estimation results between the constrained methods and the proposed method. In particular, the apnea diagnostic ability at a fixed AHI threshold of the proposed method performed better in relation to the sensitivity, specificity, kappa statistics, and area under the ROC than the other methods with a PVDF sensor [37, 82]. Moreover, the greatest disadvantage of these previous systems was the necessity for the subject to wear or attach the PVDF sensor to their body or face during sleep, which could interrupt their normal sleep architecture.

2.4.3. Validation of PVDF Film Sensors

In this study, the PVDF sensors were uniformly oriented under the subject's back position in a particular direction. To ensure the validity and reliability of the respiratory signal measurements, the PVDF sensors were aligned horizontally as shown in Figure 2-1, because subjects tend to move more often from side to side than in the longitudinal planar direction (up and down) during sleep. Sensors that are similar in shape and size to proposed one can easily be found in several commercialized sleep monitoring devices. For example, SleepScan SL-501™ (TANITA; Tokyo, Japan) is a device that collects numerous kinds of physiological signals during sleep, including the pulse rate, respiratory rate, and body motion data, and it is designed to be long in the horizontal direction. Other analogous examples

are the EarlySense System™ (EarlySense; Massachusetts, USA) and Nemuri (which means “Sleep”) SCAN NN-1300™ (PARAMOUNT BED; Tokyo, Japan). Using PVDF sensors, not only respiratory signals, but also BCG signals could be measured (Figure 2-2). Moreover, when the PVDF sensor was aligned horizontally, the best signal-to-noise ratio (SNR) for the BCG signal was revealed in the preliminary test. It is speculated that blood ejection-induced vibration was transferred more strongly along a particular axis to the sensor through the bed mattress during the recording.

2.4.4. Validation of Sleep Apnea Detection Algorithm

During PSG recording, the respiration patterns were different for the various subjects and varied depending on the position in bed and the sleep posture. To consider these things, adaptive thresholds were set based on the standard deviation of the PVDF signals for every minute for each subject in the apnea detection algorithm. As a result, accurate AHI estimation results could be obtained compared with PSG AHI. However, proposed method tended to underestimate apneic events at higher AHI level, as shown in Figure 2-5(a) and (b). At this level, apneic events occurred frequently in a short period, and the apneic event detection was ineffective under these conditions. In this study, the apnea detection algorithm was developed based on a “fixed time window” in consideration of real-time processing for ambulatory or home monitoring purposes. Apnea can persist for more than 30 s (1 epoch) in patients with severe apnea, and these durations can be diagnosed as normal breathing in the algorithm because the apnea threshold was set based on a change in the standard

deviation of the PVDF data in the fixed time window. This is why a 60 s analysis window was used instead of 1 epoch, which is the most widely used time scale in sleep studies. Despite these efforts, the increased baseline of the threshold due to the restricted time window made it difficult to detect consecutive multiple apneic events.

In contrast, proposed method tended to overestimate apneic events at the lower AHI level. One could speculate that it may misestimate a respiratory signal drop as an apneic event that does not meet the standard scoring criteria. Moreover, other SRBD such as snoring, respiratory event-related arousals (RERAs), upper airway obstruction, and Cheyne-Stokes breathing could occur in patients with sleep apnea [25]. These can also influence the amplitude decrease in the respiratory signals and might be estimated to be sleep apnea or hypopnea in the system. Moreover, PVDF signals may be distorted by motion artifacts that cannot be removed completely from the analysis process, which is one of the reasons that algorithm overestimates apneic events at a lower AHI. Despite these shortcomings, the overall apnea detection performance showed a high relationship between AHIs ($R = 0.94$).

In addition, as shown in Table 2-5, the sensitivity was significantly lower than the specificity in the normal and mild severity groups. In these groups, the apnea detection sensitivity could be reduced considerably by only a few wrong estimates because the percentage of sleep apnea occurrences was markedly less than that of normal breathing. Thus, the kappa statistic was also used to evaluate the apnea detection performance. In particular, the difference between the sensitivity and specificity of the normal group was approximately 10% less than that of the moderate

severity group, but there was no difference between the overall kappa statistics. Therefore, it could be concluded that the proposed method showed similar apnea detection performances in all of the groups. In this study, the algorithm performed poorly when subjects slept in a lateral posture. During the respiratory cycle, respiration-induced vertical (frontal axis) pressure was effectively transferred from the body to the PVDF sensors in a supine or prone posture. However, respiration-related vertical pressure was transferred horizontally to the PVDF sensor in the lateral posture, and the respiratory signal measured by the sensor was significantly attenuated or distorted. As a result, the apnea detection performance in the lateral posture was relatively low and reflected a trade-off between detection accuracy and unconstrained monitoring.

CHAPTER 3. SNORING DETECTION

3.1. Methods

3.1.1. Participants and PSG Data

Twenty OSA patients participated in this study, and overnight PSGs were conducted at SNUH Center for Sleep and Chronobiology. On the basis of the standard PSG routine [54], data were collected from an EEG; bilateral EOG; EMG from the mandible and bilateral tibialis anterior muscles, oronasal airflow, abdominal and thoracic movement; lead II ECG; SpO2; body position; and a reference snoring signal from a piezoelectric vibration sensor (Cadwell, Kennewick, WA, USA) placed on the neck. Snoring signals from the PVDF sensor were simultaneously recorded with the PSG data. All of the signals were collected using a NI-DAQ 6221 (National Instruments, Austin, TX, USA) device with a 250 Hz sampling frequency. After PSG recording, sleep stages and associated events including sleep apnea were scored by a registered PSG technologist according to the established criteria [54]. Table 3-1 summarizes the parameters related to the subjects and PSG results.

Table 3-1. Sleep related parameters of subjects for snoring detection.

Parameters	
Gender (Male/Female)	17/3
OSA severity (Mild/Moderate/Severe)	1/7/12
Parameters	Mean ± S.D
AHI (events/h)	41.8±19.3
Age (years)	49.4±13.6
BMI (kg/m^2)	28.2±3.7
Sleep latency (min)	6.2±4.0
Stage N1 & N2 (%)	63.7±9.9
Stage N3 (%)	4.5±7.0
Stage REM (%)	16.7±4.9
Total sleep time (h)	8.1±0.5
Sleep efficiency (%)	86.1±8.0

S.D.: standard deviation; AHI: apnea hypopnea index; BMI: body mass index; REM: rapid eye movement; N: non-REM sleep

3.1.2. Feature Extraction for Snoring Event Detection

The study about an unconstrained snoring detection was published as a journal paper [84]. As shown in Figure 3-1, the signal outputs of the PVDF sensor include three types of physiological signals, including respiration, BCG, and snoring [84]. During snoring occurrences, the vibration of respiratory structures caused by the obstructed air movement was detected by the PVDF sensor, and the output signals of the sensor reflected the snoring of the subjects. When snoring occurred, the sensor signal was relatively noisy and had no standard waveform compared to the other bio-signals. Thus, this study used spectral features to distinguish snoring events from normal breathing, body movement, or other physiological signals.

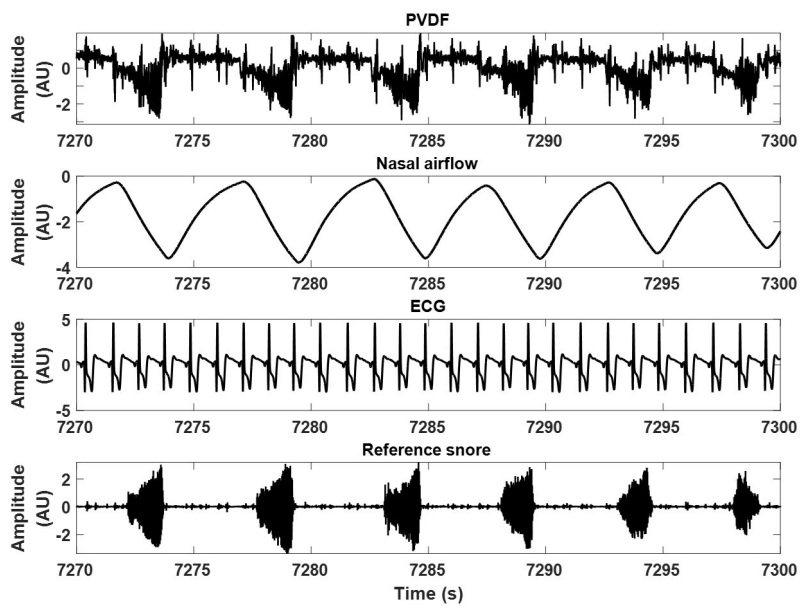

Figure 3-1. Signal output from the PVDF sensor for snoring detection.

The unprocessed data from four channels were averaged and band-pass filtered with a pass band of 10 to 100 Hz, which is the recommended filter band for snoring recordings from the AASM manual [54]. The data were also notch filtered at 60 Hz to remove power line noise. After filtering, two spectral features were extracted using a short-time Fourier transform (STFT). The STFT is expressed as follows:

$$\mathbf{X[n,k]} = \sum_{m=0}^{L-1} x[n+m]w[m]e^{-j\left(\frac{2\pi}{N}\right)km} \quad \textbf{(3-1)}$$

where n is the sample number, $x[n]$ is the filtered PVDF data, $w[m]$ is the 128 point sliding Kaiser window function, k is the frequency index, and L is the length of the analysis window. The STFT analysis was conducted using a 256 fast Fourier transform (FFT) length with 10 overlapping samples. The type and length of the sliding window, FFT length, and overlapping samples were set experimentally. Figure 3-2 shows the band-pass filtered PVDF signals and their spectrograms during snoring without movement, snoring with movement, breathing without movement, and breathing with movement [84]. As shown in Figure 3-2(a) and (b), when snoring occurred, the PVDF spectrum included significant frequency components and peak frequency of over 25 Hz, whereas these frequency characteristics did not occur during movement or breathing, as shown in Figure 3-2 (c) and (d). In this figure, dashed lines in the spectrograms indicate 25 Hz and dashed squares indicate body movement occurrences.

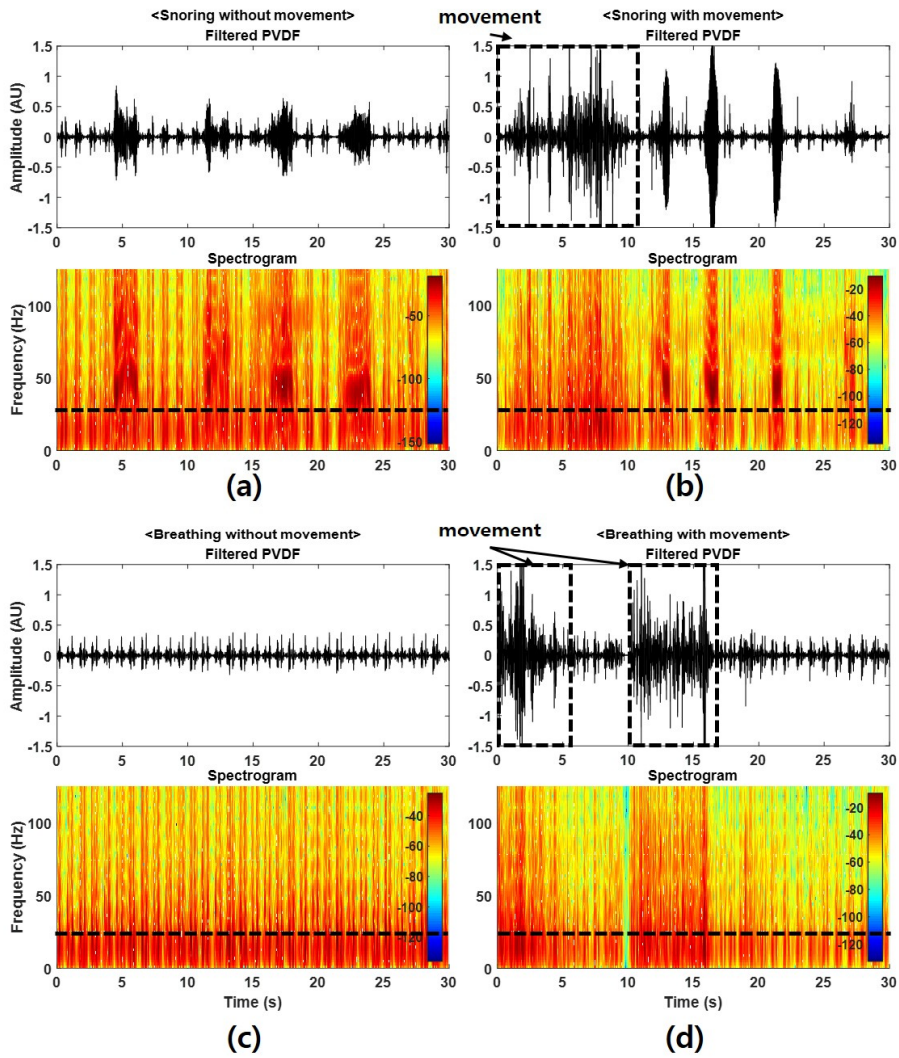

Figure 3-2. Band-pass filtered PVDF signals and their spectrograms.

Additionally, previous literature reported that PVDF signals containing periodic components with fundamental peak frequency from 20–30 Hz to approximately 250–300 Hz were manually scored as snore events [83]. With these criteria, the following two spectral features were selected to detect snoring events. The first spectral feature was the power ratio (PR), which is the ratio of the sum of power produced at greater than 25 Hz to the sum of power produced at less than 25 Hz.

$$\boldsymbol{PR_n = \sum_{k=27}^{k=N-1} X[n,k] / \sum_{k=0}^{k=26} X[n,k]} \qquad \textbf{(3-2)}$$

The other feature was peak frequency (PF), which is the maximum value among the frequency (k) values in each fixed time (n), as described by (3-3).

$$\boldsymbol{PF_n = k_{max},} \qquad \textbf{(3-3)}$$

$$\textbf{where } \boldsymbol{|X[n,k_{max}]| = max|X[n,k]|}$$

Examples of the PR and PF are shown in Figure 3-3 [84]. As shown in the Figure, there were no significant changes in either PR or PF when body movement occurred, whereas both increased during snoring. After feature extraction, PR and PF were used as the input to the support vector machine (SVM) for classification. In this study, only these two spectral features were used to establish a fast and simple snoring detection algorithm.

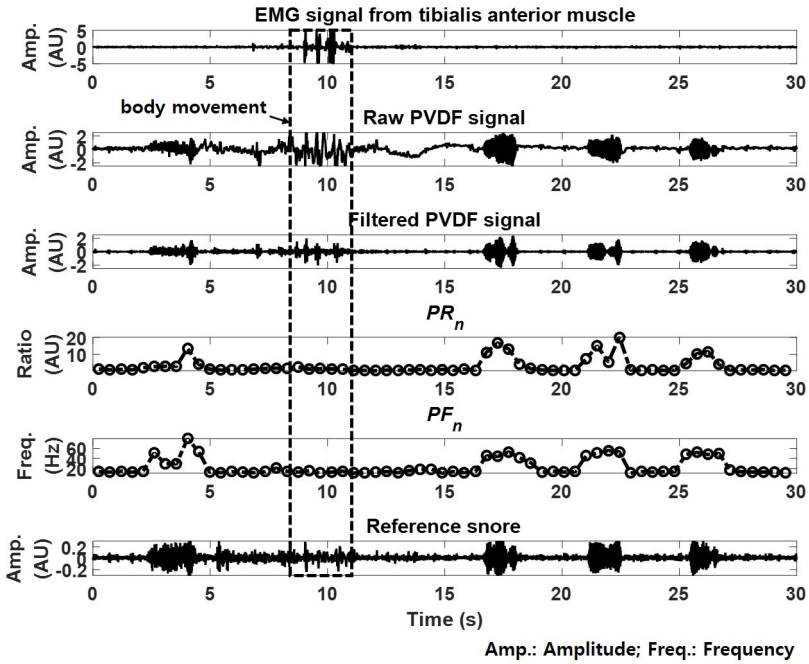

Figure 3-3. Spectral features of the PVDF data.

3.1.3. Data Selection and Reference Snoring Labelling

To establish the snoring detection algorithm, 50 epochs of PVDF data composed of 20 "snoring" (SN), 20 "snoring with movement" (SM), and 10 "normal breathing" (NB) epochs were randomly selected for each subject (total 1000 epochs of data). The descriptions of the SN, SM, and NB epochs are:

SN: only snoring occurred in an unmoving state

SM: both snoring and body movement occurred

NB: normal breathing without snoring

In this study, the EMG signal from the tibialis anterior muscle was applied as a reference for assessing body movement. If the output voltage of the EMG signal exceeded 4.5 V (almost saturated), the signal was scored as body movement.

Because there is no clear definition for a "snoring event," reference snoring events were visually and aurally observed by three healthy human observers without any recognised auditory impairments. First, each observer saw only the reference snoring signal waveform from the PSG snoring sensor on an LCD monitor (SyncMaster T240HD, Samsung, Korea) to confirm the snoring events. A consensus was reached if each observer's labelling concurred within 1 s of each other, and the labelling results from all of the observers were combined into a single label by applying a logical AND operation. In other words, the overall event result became a non-snore if at least one the observers scored the data as a non-snore. For events on which the observers did not concur, the observers reconfirmed the events by listening to the converted audio files using headphones (EH-150, Sennheiser, Germany). The results of each observer's labelling process were not revealed to the other observers.

3.1.4. Snoring Event Classification Based on the SVM

The SVM is a supervised machine learning model used for classification or regression analysis. The SVM constructs a maximum margin hyperplane between the two classes, and the support vectors indicate the feature points that are closest to the hyperplane [92]. An equation of the separating hyperplane for binary classification can be described as

$$\mathbf{d}(\mathbf{x}) = \mathbf{w} \cdot \mathbf{x} + \mathbf{b}, \quad \mathbf{class}(\mathbf{z}) = \mathbf{sign}(\,\mathbf{d}(\mathbf{x})\,) \qquad \textbf{(3-4)}$$

where **x** is the feature vector, **w** is the normal vector to the hyperplane, • denotes the dot product, and *b* is the bias. Through the machine learning process, the margin maximizing values of **w** and *b* are obtained. The SVM can be effectively applied to nonlinear classification by mapping the feature data into higher dimensions, where it exhibits linear patterns, which is called the "kernel trick" [93]. Therefore, the selection of the proper kernel function is critical because classification performance can vary for the same data. To generalize and simplify the algorithm, a linear kernel function of the SVM was used in this study. Figure 3-4 shows the distribution of the sample data in the feature space before (a) and after (b) transformation using the linear kernel function [84]. As shown in Figure 3-4(b), snore classes were separated from the other classes by the hyperplane of the SVM in the transformated space. Figure 3-4(c) shows enlargement of dashed rectangular box in Figure 3-4(b).

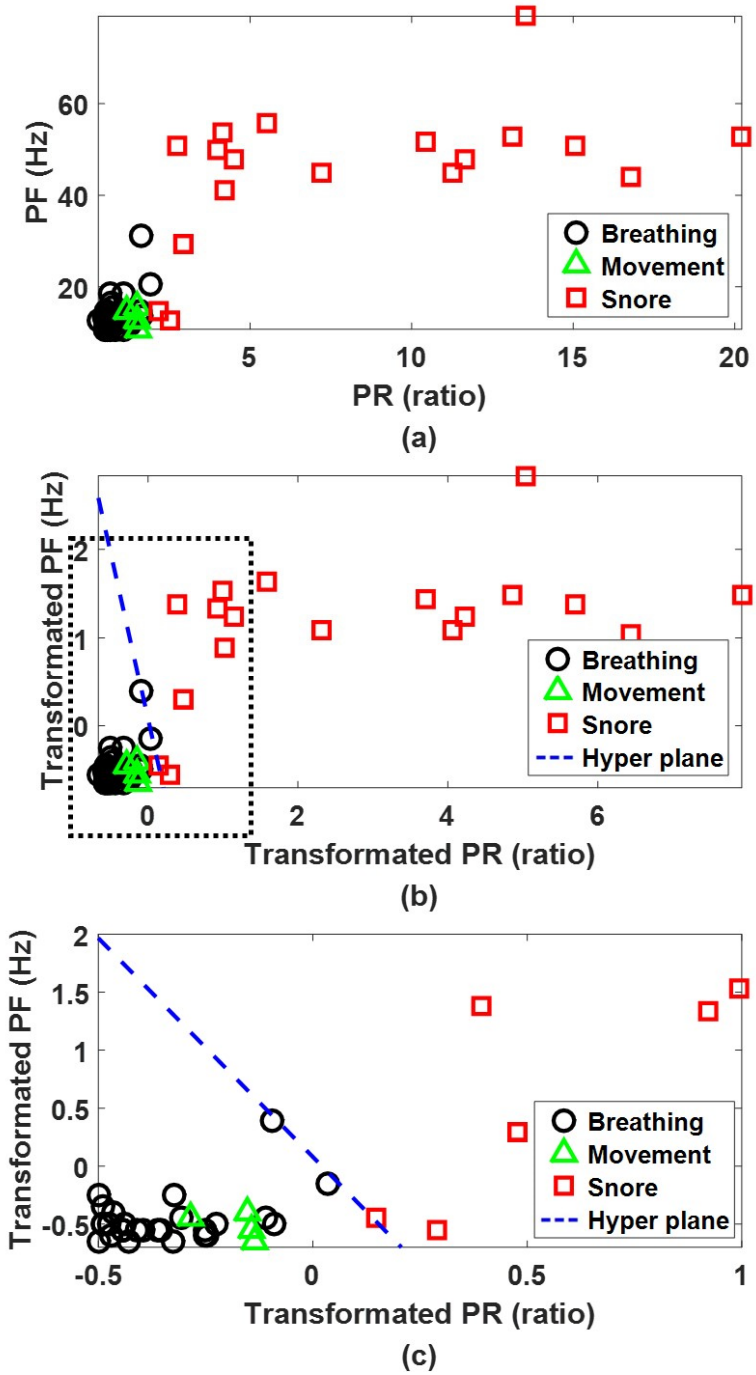

Figure 3-4. Scatter plot of three categorized classes in the feature space.

Using the SVM classification, each result was first classified into two categories: “snore” or “non-snore.” In this study, non-snore events included all but the snore events, including normal breathing, body movement, and silence. Finally, two post-processing steps were conducted to prevent overestimation of the snore events. First, a snore event decision was made if there were two or more consecutive snore events. Second, if two distinct snore events occurred within 1 s, they were considered together as a single snoring event. All snoring detection procedures are shown schematically in Figure 3-5 [84]. Process was performed with the following steps: 1) extraction of the snoring signal; 2) extraction of spectral features; 3) classification of snore events; 4) performance evaluation.

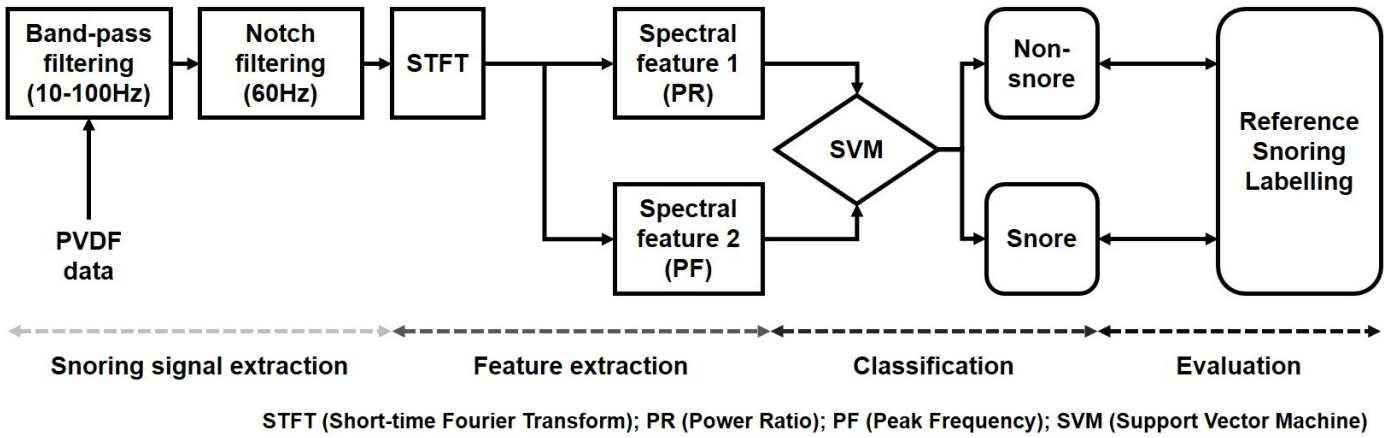

Figure 3-5. Snoring detection procedure.

3.2. Results

3.2.1. Event-By-Event Snoring Detection

For the validation of the algorithm, the SVM was trained and tested on the basis of the leave-one-out cross validation (LOOCV) technique. In other words, 950 epochs of data from 19 subjects were used as a training set for the SVM and 50 epochs (20 SN, 20 SM, and 10 NB) of data from one subject were selected as a test set, and this procedure was repeated 20 times for each subject. After applying LOOCV, the snoring event detection results were compared with those from the reference snoring labelling. To evaluate the performance of proposed algorithm, sensitivity and positive predictive value (PPV) were used. Sensitivity is defined as TP/ (TP + FN) and PPV is defined as TP/ (TP + FP), where TP, FN, and FP denote true positive, false negative, and false positive, respectively. In the study, TP represents the number of events correctly classified as snore events. Table 3-2 shows the SN, SM, and NB classification results for all 1000 epochs. From the Mann–Whitney–Wilcoxon test, there were no significant differences in the sensitivity ($p = 0.461$) and PPV ($p = 0.072$) values between the SN and SM results from proposed method and those from the reference labelling.

Examples of snore event detection for the SN, SM, and NB epochs are shown in Figure 3-6 [84]. As shown in Figure 3-6(b), snore-related PVDF data were correctly classified as snore events whereas body movement events were correctly classified as non-snore events.

Table 3-2. SN, SM, and NB classification results for all epochs.

	SN	SM	NB	Total
TP	2050	1342	0	3392
FN	104	88	0	192
FP	33	38	15	86
Sensitivity (%)	95.2	93.8	-	94.6
PPV (%)	98.4	97.2	-	97.5

SN: snoring; SM: snoring with movement; NB: normal breathing;
TP: true positive; FN: false negative; FP: false positive;
PPV: positive predictive value

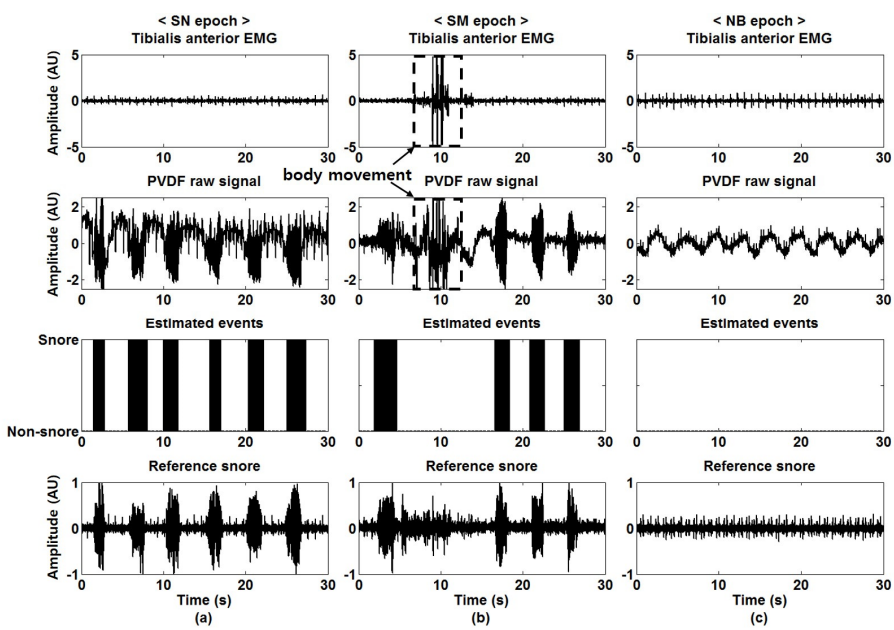

Figure 3-6. Snore event detection for SN, SM, and NB epochs.

Table 3-3 shows a comparison between the snore event detection results from the proposed method and those from previous studies. The snore event detection sensitivity from the ambient microphone-based methods had lower performance (1.5%-12.4%) compared with the proposed one [55, 56, 58, 59], except for one case [57]. In other studies, air mattress [61] and piezo snoring sensor based [62] methods showed a slightly lower sensitivity than the proposed method.

Table 3-3. Comparisons of snoring detection results with previous studies.

Author (year)	Sensor	Class	N	Labelling	Sensitivity (%)
Duckitt (2006)	Mic	Snore/ others	6 snores	Manually	82.2
Cavusoglu (2007)	Mic	Snore/ non-snore	18 snores, 12 OSA	ENT specialist	90.2
Yadollahi (2010)	Mic (ambient) Mic (tracheal)	Snore/ breathing	23 OSA	Auditory & visual	94.8 98.3
Shin (2010)	Air mattress	Snore/ breathing	6 normal	Simulation	93.0
Azarbarzin (2011)	Mic (ambient) Mic (tracheal)	Snore/ non-snore	7 snores, 23 OSA	Auditory & visual	93.1 98.6
Emoto (2012)	2 Mic	Snore/ breathing	4 normal, 4 OSA	Listening	89.2
Lee (2013)	Piezo snoring	Snore/ silence	21 OSA	Technician	93.3
Hwang (2015)	**PVDF**	**Snore/ non-snore**	**20 OSA**	**Auditory & visual**	**94.6**

OSA: obstructive sleep apnea; ENT: ear-nose-throat; Mic: microphone

3.2.2. Snoring Event Detection and Sleep Posture

Snoring detection performance was also evaluated by sleep posture. During PSG, the sleep posture of each subject was obtained using a sleep position sensor (SPL Lite, Pro-Tech, USA). The sleep position sensor provided four categories of posture (supine, prone, right lateral, and left lateral). After SVM classification, snoring detection results were classified according to the sleep posture, as shown in Table 3-4. A Kruskal–Wallis one-way analysis of variance (ANOVA) test [94] was then used to assess the difference in results between different postures; there were no significant differences in the sensitivity ($p = 0.194$) and PPV ($p = 0.649$) values.

Table 3-4. Snoring detection performance based on sleep postures.

	Supine	Right	Left	Prone
No. of epochs	657	90	52	1
Sensitivity (%)	94.6	95.0	94.0	-
PPV (%)	97.9	98.4	97.5	-

Right: right lateral; Left: left lateral; PPV: positive predictive value

3.2.3. Epoch-By-Epoch Snoring Detection

Snoring detection performance was also evaluated using one entire night of PVDF data. Overnight data from 10 randomly selected participants (out of 20 total participants) were subjected to epoch-by-epoch analysis. For the analysis, if snoring events occurred more than once in one epoch of PVDF data, that epoch was considered to be an "estimated snore epoch." The same rule was applied to reference snore signals, and epoch-by-epoch statistical analysis between the "estimated snore epoch" and a "reference snore epoch" was performed. The epoch-by-epoch results are shown in Table 3-5. A kappa statistical analysis revealed a borderline case between almost perfect ($0.8 < k < 1$) and substantial agreement ($0.6 < k < 0.8$), whereby the overall $k = 0.8$ [90]. Figure 3-7 shows the snore epoch estimation results for the best case (Figure 3-7(a), subject #2) and the worst case (Figure 3-7(b), subject #1) [84]. In the best case, the sensitivity, specificity, accuracy, and kappa statistic were 98.3%, 86.0%, 94.9%, and 0.87, respectively. In the worst case, the corresponding values were 95.9%, 75.8%, 87.6%, and 0.74, respectively.

Table 3-5. Epoch-by-epoch snoring detection.

No. of epoch	Sensitivity (%)	Specificity (%)	Accuracy (%)	Kappa statistic
953±62	95.7±3.6	84.2±5.9	91.2±2.1	0.80±0.04

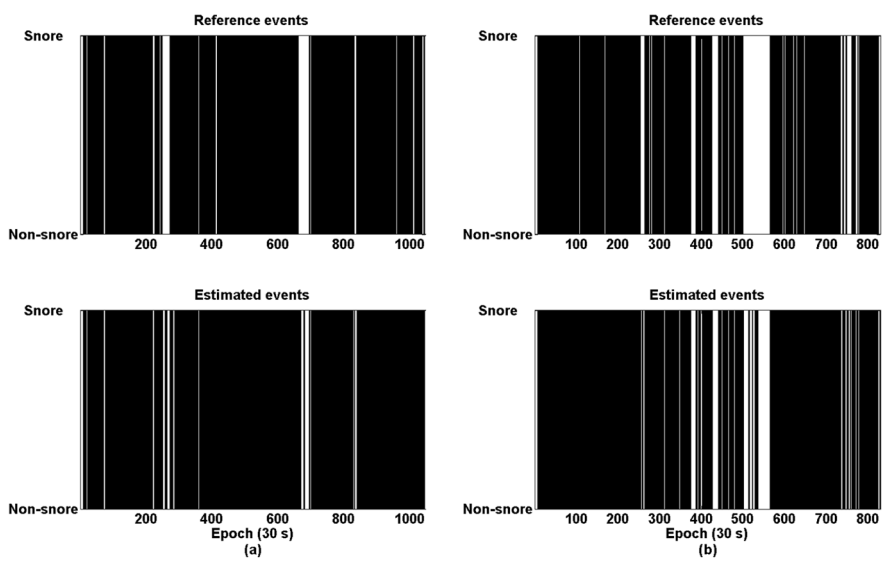

Figure 3-7. Epoch-by-epoch snore detection results for the best and worst cases.

3.3. Discussion

3.3.1. Agreement between Proposed Method and Reference Snoring

The snoring event detection process was performed with the following steps: 1) extraction of the snoring signal from the PVDF data; 2) extraction of spectral features using STFT; 3) classification of snore events with training of the SVM classifier. For algorithm evaluation, LOOCV was adopted, and it was shown that the detected snore events strongly concurred with those from the reference snore signals. As a result, a total of 3392 snore events were correctly detected using the proposed method. In the epoch-by-epoch analysis (Table 3-2), for all participants, the kappa statistic was greater than substantial agreement ($k > 0.6$). In addition, more than half (6 of 10) of the participants exhibited almost perfect agreement ($k > 0.8$); thus, the overall k was in a borderline case between almost perfect and substantial agreement [90]. Consequently, it can be concluded that proposed method can be used for snoring detection in a sleep monitoring system.

3.3.2. Comparisons with Previous Studies

The proposed snoring detection method had a higher or similar performance compared with previous microphone-based or constrained PVDF based methods (Table 3-3). For example, Duckitt *et al.* used a freestanding microphone to monitor snoring automatically on the basis of hidden Markov models (HMMs), and the results were compared with manually obtained annotations [58]. That method classified snore events with 82.2% sensitivity, which was approximately 10% lower

than results from this study and was vulnerable to detecting a snore in regular breathing sounds or ambient noises. Cavusoglu *et al.* used a microphone that was placed over the subject's head to detect snoring episodes for simple snorers and OSA patients[59]. An analysis accounting for ambient noise during sleep was not conducted in that study, and snoring detection performance was lower than that of the proposed one in OSA patients.

Yadollahi *et al.* used two microphones, one placed over the trachea and the other hung in the air (ambient microphone) to distinguish the normal breathing and snore sounds [57]. Azarbarzin *et al.* also used two microphones (tracheal and freestanding) to extract the snore sound from the respiratory sound signals of simple snorers and OSA patients [56]. In both of those studies, better snoring detection performance was observed when data from tracheal sound recordings were used. However, for tracheal sound recordings, the microphone must be attached or placed over the trachea, and this can cause a great deal of disturbance and inconvenience to sleeping subjects. In addition, noise or vibration caused by body movement could be an important issue for tracheal sound recordings; nevertheless, this was not considered in either study. Emoto *et al.* used a matched pair of microphones for breathing and snoring episode detection in sleep sounds [55]. Although they used only eight subjects' data and two microphones, the overall snoring detection sensitivity was approximately 5% lower than results of this study.

In other previous studies, Shin *et al.* used an air mattress with a balancing tube as a snoring detection sensor [61]. Although they were able to monitor snoring events on

the basis of an unconstrained measure, the subjects were instructed to simulate snoring while awake to validate the detection algorithm, and no simple snorers or OSA patients participated in the experiment. Lee *et al.* also used a piezoelectric sensor in order to establish a snoring detection method based on HMMs [62]. However, the sensor used in their experiments was attached to the neck during an overnight PSG recording, and this could affect the subjects' normal sleep because of the inconvenience of the direct electrode attachment. The proposed method showed better performance, as well as the convenience of unobtrusive measurements compared to the piezoelectric sensor method.

Norman *et al.* analysed 62 subjects' PSG data to evaluate the Sonomat, which uses a PVDF film sensor, with regard to its capability for diagnosing SRBD, and they verified that the Sonomat can be a reliable device for the detection of snoring events [83]. However, although they used a PVDF sensor for snoring detection, all Sonomat events were manually scored in the same manner as PSG scoring because the focus of their research was the validation of the sensor. Object of this study was focused on the development of a method for snoring detection using a PVDF sensor.

3.3.3. Validation of the Snoring Detection Algorithm

In the previous studies using PVDF films as nonintrusive physiological sensors, motion artifacts were considered an important issue because the films are sensitive to minute movements and external vibrations [76, 80]. In this study, an accurate snoring detection method robust to the occurrence of motion artifacts was established.

From Table 3-2, the proposed method classified snore events with an average sensitivity of over 90%, and PPV of over 95%, for both “snoring” and “snoring with movement” epochs. Furthermore, there was no significant difference in the snore event detection results between the SN and SM epochs. One could speculate that the two selected spectral features (PR and PF) were proper features for snore event detection and motion artifact event rejection. The frequency band of the motion artifact was relatively low compared to that of snoring, and acceptable results for each SN and SM epoch were able to obtained using this spectral information.

SVM was originally designed for binary classification and is known to perform best for two group classification problems [92, 95, 96]. Based on the previous researches, SVM was selected, rather than other possible classifiers such as the HMM or artificial neural network, for the binary classification of snore/non-snore events. As a result, only two spectral features and a linear SVM classifier were used to establish a simple, fast, and generalized snoring detection algorithm. Two complementary spectral features were selected, and proposed method was able to correctly classify snore events with 94.6% sensitivity, despite using only two simple features.

With regard to the sampling rate of the analysis data, the snoring-related vibration from a PVDF sensor can be measured with a 250 Hz sampling rate, whereas the microphone-based studies that were referenced in this study required at least a 10 kHz sampling rate for snoring sound recording, which may be unsuitable for residential or ambulatory monitoring devices. Quantitatively, proposed method required approximately 4.5 s to process one entire night (approximately 8 h) of

PVDF data, whereas a previous microphone-based study required approximately 6 min to process 6 h of data[59]. Less than 5 s can be considered as an acceptable processing time for the data from one entire night.

Proposed method tended to overestimate snore events in the epoch-by-epoch analysis (Table 3-5, and Figure 3-7). It is considered that algorithm does not entirely reject motion artifacts that influenced the PVDF signals. As shown in Figure 3-4(c), spectral features during body movement were relatively close to the SVM hyperplane, relative to those from normal breathing. This means that body movement can be more easily misclassified as a snore event in some SVM classifications. In addition, wakefulness during sleep can be related to misclassification of non-snore events because wakefulness is similar to a motion artifact. Another suitable feature that could be selected for motion artifact or wakefulness detection, such as a motion-related frequency band (relatively low-frequency), may improve method's accuracy for 'real' snoring detection. Alternatively, one could speculate that the proposed method may have misclassified non-detectable levels of snoring signals that were not noted by the observers. Despite these deficiencies, the average snore epoch detection accuracy for one entire night of data was over 90%, and it can be regarded that almost all motion artifact periods were effectively excluded in the analysis process.

During sleep, snoring signal patterns can vary depending on the subject or sleep posture [97]. To consider these aspects, the snoring detection algorithm was analysed according to three sleep postures (supine, left and right lateral), and there were no

significant differences in the snore event detection results among these sleep postures (Table 3-4). From the PVDF data, there was only one snoring or non-snoring epoch of prone posture, and it can be concluded that it is difficult to sleep in a prone posture during PSG because many electrodes are attached to the subject's face and body.

CHAPTER 4. SLEEP STAGES DETECTION

4.1. Methods

4.1.1. Participants and PSG Data

Eleven healthy subjects and thirteen OSA patients participated in this experiment. Nocturnal PSG was conducted at the SNUH Center for Sleep and Chronobiology. All of the PSG data were collected based on the following standard PSG routine [54]: EEGs at the C3-A2 and O2-A1 positions based on the international 10–20 system, EMGs from the chin and bilateral tibialis anterior muscles, bilateral EOGs, lead II ECG, nasal airflow, abdominal and thoracic movements, snoring, and SaO2. The sleep stages were scored by a registered PSG technologist according to the criteria developed by the AASM [54]. Based on the AHI (events/hour) results, three mild, nine moderate, and one severe OSA patients were determined. A summary of the parameters related to the subjects and PSG results is presented in Table 4-1.

To develop a sleep stages detection method for PVDF data, data from five subjects (approximately 20%) with a normal to severe OSA were randomly selected as a training set. To evaluate the algorithm performance, an epoch-by-epoch sleep stages detection was conducted for 19 test datasets, and the results were compared with those from the PSG.

Table 4-1. Sleep related parameters of subjects for sleep stages detection.

	Normal	OSA
N	11	13
AHI (events/hour)	1.3±0.9	21.5±9.3
Gender (M/F)	7/4	8/5
Age (years)	38.6±19.9	50.2±15.3
BMI (kg/m^2)	23.5±1.7	25.9±3.2
Sleep latency (min)	13.6±11.7	9.8±9.6
Stage Wake (%)	18.7±10.0	14.1±8.2
Stage N1 & N2 (%)	57.5±12.2	63.4±6.9
Stage N3 (%)	9.6±9.2	5.6±5.3
Stage REM (%)	14.3±4.5	16.9±4.5
Total sleep time (h)	8.4±0.4	8.2±0.5
Sleep efficiency (%)	82.4±9.8	85.9±8.2

OSA: obstructive sleep apnea; N: number of participants;
AHI: apnea hypopnea index; BMI: body mass index; REM: rapid eye movement

Figure 4-1 shows the signal output from the PVDF sensor for several physiological signals, including respiration, BCG, and body movement at the start of PSG and middle of the night. However, Figure 4-1 shows that the BCG signal quality was not kept constant because it could be easily influenced by the sleep position or contact problem. Poor BCG signal quality can be a limitation for the HRV based sleep staging method. On the other hand, the PVDF data continuously reflected the respiratory-related signal of a subject during an overnight PSG recording. Thus, this study used respiration and body movement signal for reliability of the sleep stages estimation method.

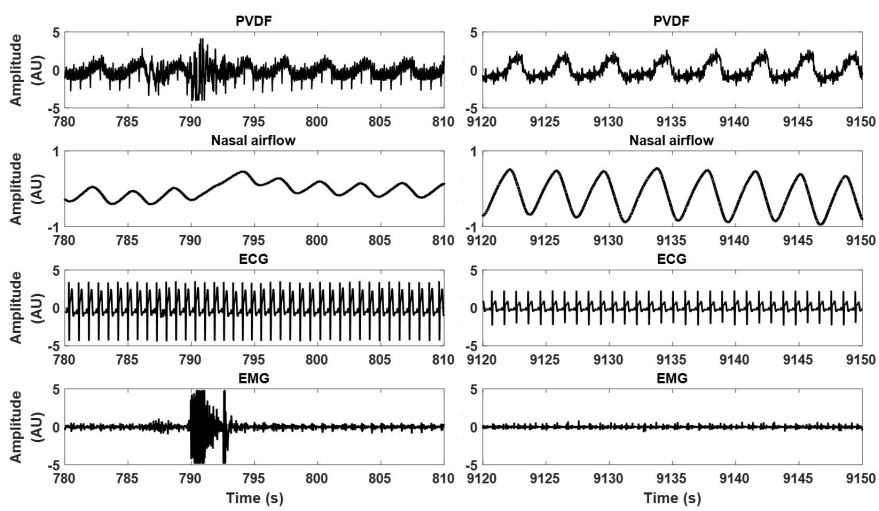

Figure 4-1. Signal output from the PVDF sensor for sleep stages detection.

4.1.2. REM Sleep Detection

In a previous study, a method for estimating REM sleep using the dynamics of the respiratory signal from a thermocouple sensor was reported [98]. In this study, that algorithm was modified to estimate REM sleep based on the average rate and variability of a respiratory signal unconstrainedly measured using the PVDF sensor [99].

First, the process of extracting the common respiratory components reflected in the four channels of the PVDF data was conducted. The PVDF data of each channel were normalized to have zero mean and unit variance, and PCA was applied to the normalized PVDF data to extract the principal components. Thereafter, to obtain a common respiratory feature between the four data channels, PC1 was extracted and band-pass filtered with a passband of 0.1–0.5 Hz.

Second, the average respiratory rate of each epoch (30 s) was determined using an autocorrelation method [98]. The equation of the autocorrelation method can be described as follows:

$$\boldsymbol{R_{xx}(\tau) = \frac{1}{N}\sum_{m=0}^{N-\tau-1} s[m]s[m+\tau]} \qquad \textbf{(4-1)}$$

where $\boldsymbol{R}$, $\boldsymbol{N}$, $\boldsymbol{\tau}$, and $\boldsymbol{s}$ denote the autocorrelation, total number of samples in an epoch, time delay, and respiratory signal from PC1, respectively. By detecting the first peak of the autocorrelation function, the average respiratory rate of each epoch was obtained using the following equation:

$$f_{rate} = f_s / \tau_{peak} \quad \textbf{(4-2)}$$

where f_{rate} denotes the estimated respiratory rate, f_s denotes the sampling rate of the signal, and τ_{peak} denotes the delay of the first peak of the autocorrelation, respectively.

Third, the parameters and thresholds for the REM sleep estimation were calculated [98]. The descriptions for these parameters and thresholds are given in Table 4-2. As a smoothing technique, the "robust locally weighted regression" method was selected among the smoothing methods available in the MATLAB software (MathWorks Inc., USA, R2015a version). This method is a type of weighted linear least square regression, and it can be described as follows:

$$\mathbf{S} = \sum_{i=1}^{M} W_{ii} r_i^2 \quad \textbf{(4-3)}$$

where W is a weight matrix, and r is the average respiratory rate [100].

To modify an existing algorithm for the PVDF data, the data from five subjects (approximately 20%) with normal to severe OSA were randomly selected as a training set. As a result of the training procedure, the length of the smoothing window was changed from 300 epochs (9000 s) to 250 epochs (7500 s). Figure 4-2 shows respiratory rate and smoothed rate of subject during whole night of sleep (Figure 4-2(a)), absolute difference of rate and smoothed absolute difference of rate (Figure 4-2(b)), smoothed rate and adaptive threshold 1 (Figure 4-2(c)), and smoothed absolute difference of rate with two different threshold levels (Figure 4-

2(d)). In this figure, gray regions indicate REM sleep epochs scored by a sleep physician.

Table 4-2. Parameters and thresholds for REM sleep detection.

Parameters	Description
Respiratory rate	Average respiratory rate in an epoch obtained by the autocorrelation method
Smoothed rate	Smoothed value of 'respiratory rate' with 30 epochs (900 s)
Absolute difference of rate	Absolute value of 'respiratory rate' – 'smoothed rate'
Smoothed absolute difference of rate	Smoothed value of 'absolute difference of rate' with 30 epochs (900 s)
Thresholds	**Description**
Fixed threshold	Mean value of 'smoothed absolute difference of rate' for all training set during non-REM sleep (=0.4)
Adaptive threshold 1	Smoothed value of 'respiratory rate' with 250 epochs (7500 s) + 'fixed threshold'
Adaptive threshold 2	Smoothed value of 'absolute difference of rate' with 250 epochs (7500 s)

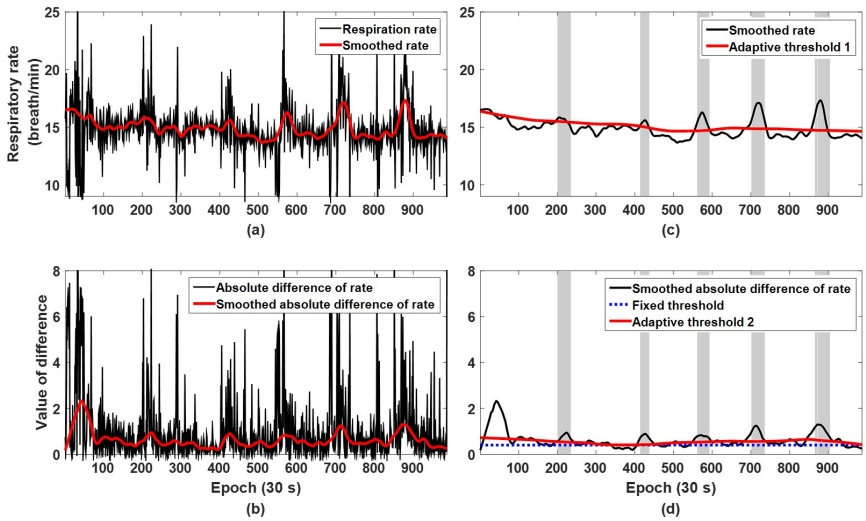

Figure 4-2. The parameters and thresholds for estimating REM sleep.

Finally, candidates for the REM sleep periods were selected when the parameters satisfy all the following conditions:

Condition 1: smoothed rate > adaptive threshold 1

Condition 2: smoothed absolute difference of rate > fixed threshold

Condition 3: smoothed absolute difference of rate > adaptive threshold 2

For the selected REM sleep period candidates, the final REM sleep period was determined using two post-processing methods.

Post-processing 1:

The estimated REM sleep periods during the first 60 min after sleep onset were rejected because an REM sleep period typically occurs 90–120 min after sleep onset [51].

Post-processing 2:

The estimated REM sleep periods shorter than 5 min were rejected because REM sleep tends to occur continuously [51].

All of the REM sleep detection procedures are schematically shown in Figure 4-3.

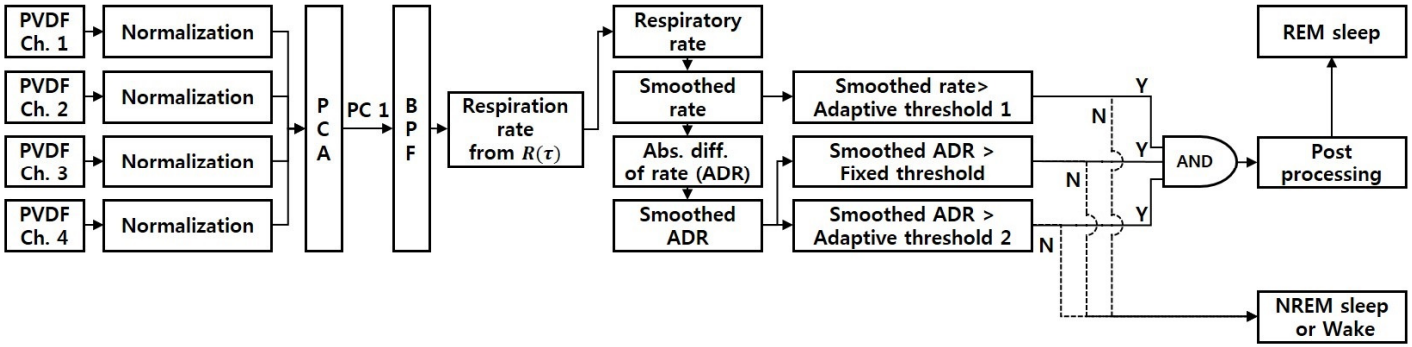

PVDF: Polyvinylidene fluoride; PCA: Principal component analysis; PC 1: Principal component 1; BPF: Band-pass filtering; $R(\tau)$: Autocorrelation method; Abs.: Absolute; diff.: Difference; AND: And function; REM: Rapid eye movement; NREM: Non-REM

Figure 4-3. REM sleep detection procedure.

4.1.3. Wakefulness Detection

Body movement signals from the PVDF data were chosen as an indicator for a wakefulness detection method. First, each channel of the PVDF data was band-pass filtered with a passband of 0.05–0.1 Hz to extract the body movement from the PVDF data. After filtering, the absolute value of each channel of the body movement signal was calculated. Feature extraction for the wakefulness detection was done by taking the square root of the product of the absolute values. This feature extraction procedure can be described by the following equation:

$$\mathbf{FW} = \sqrt{(|\boldsymbol{BM_{ch1}}| \times |\boldsymbol{BM_{ch2}}| \times |\boldsymbol{BM_{ch3}}| \times |\boldsymbol{BM_{ch4}}|)} \qquad \textbf{(4-4)}$$

where *FW* denotes the "feature for wakefulness detection," and *BM* represents the "body movement signal from each channel of PVDF data." The difference between the sleep and wakefulness *FW* from the normal subject #4 is shown in Figure 4-4. The wakefulness state is usually accompanied by a relatively high value of *FW*, as seen in the top figure. The bottom panel shows the hypnogram for comparison.

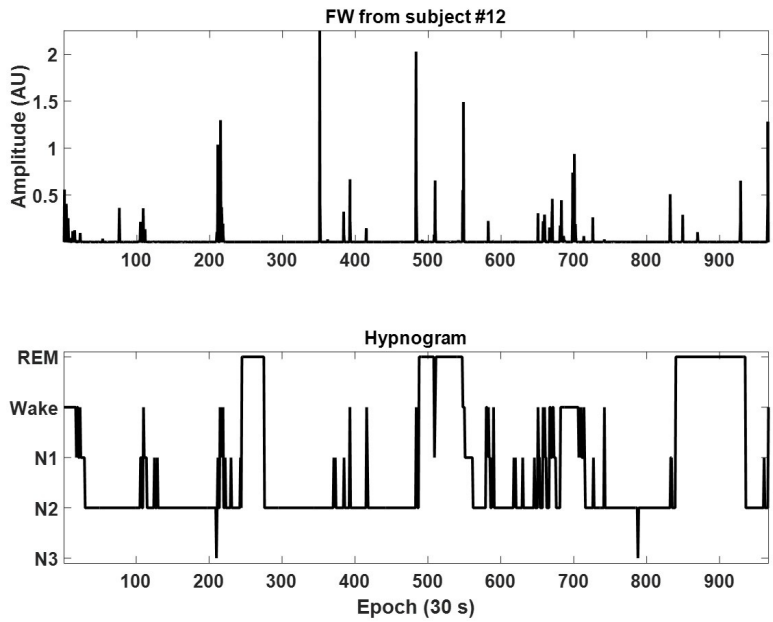

Figure 4-4. Feature for wakefulness detection and hypnogram during PSG.

After the feature extraction, the mean values of *FW* for every 30 s window were calculated for an epoch-by-epoch analysis.

$$\boldsymbol{FW_m = mean\ value\ of\ FW\ of\ the\ m-th\ epoch} \qquad \textbf{(4-5)}$$

For the wakefulness detection, FW_m was compared with the threshold for wakefulness, which is expressed as equation (4-6).

$$\boldsymbol{Threshold_{wakefulness} = 1 \times \frac{1}{N}\left(\sum_{m=1}^{N} FW_m\right),} \qquad \textbf{(4-6)}$$

N: total number of epochs

Here, the mth epoch was considered as wakefulness if FW_m exceeded the wakefulness threshold; otherwise, it was considered as sleep. The value used for the wakefulness threshold was based on the training dataset. As shown in Figure 4-5, when the value for the wakefulness detection threshold was one, the mean performance was the highest. In this analysis, Cohen's kappa (k) coefficient was marked as the "mean performance."

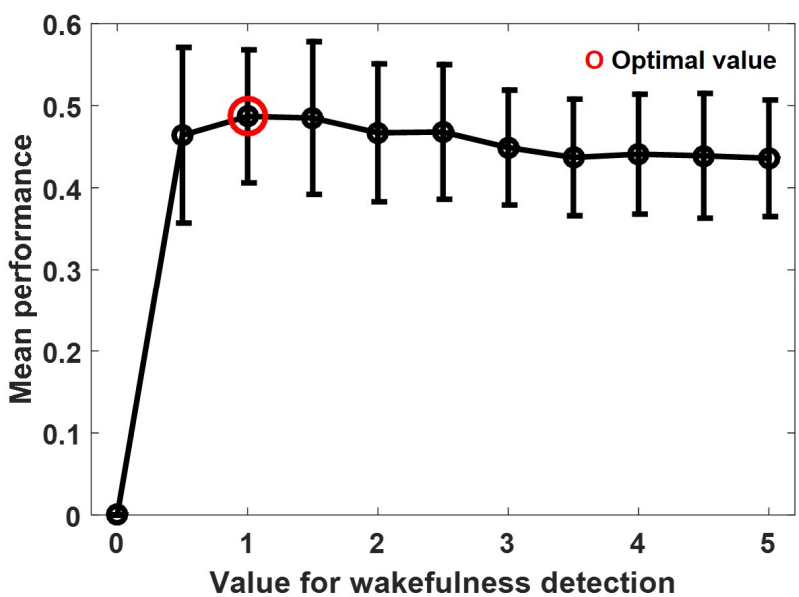

Figure 4-5. Value determination for threshold of wakefulness detection.

The final wakefulness epoch was determined using three post-processing steps.

Post-processing 3: sleep onset

The first 20 epochs (10 min) after the start of the PSG were fixed as the wakefulness epoch.

Post-processing 4: sleep offset

The end of the epoch was fixed as a wakefulness epoch.

Post-processing 5: out of bed period

Out of bed periods were determined based on the standard deviation of the respiratory signals from the PVDF data, which were used for REM sleep detection. If the standard deviation of the respiration of the *m*th epoch (σ_m) satisfied the following conditions, this out of bed period was fixed as a wakefulness epoch.

$$\textbf{if } \boldsymbol{\sigma_m < 0.1 \times \frac{1}{N}\sum_{m=1}^{N} \sigma_m}, \qquad \textbf{(4-7)}$$

$$\textbf{m-th epoch = out of bed period}$$

where *N* denotes the total number of epochs. Figure 4-6 shows an example of an estimated out of bed period and SpO2 signals from the normal subject #3. Periods with SpO2 values of less than 50% indicated actual out of bed periods during the PSG. Figure 4-7 schematically shows all wakefulness detection procedures.

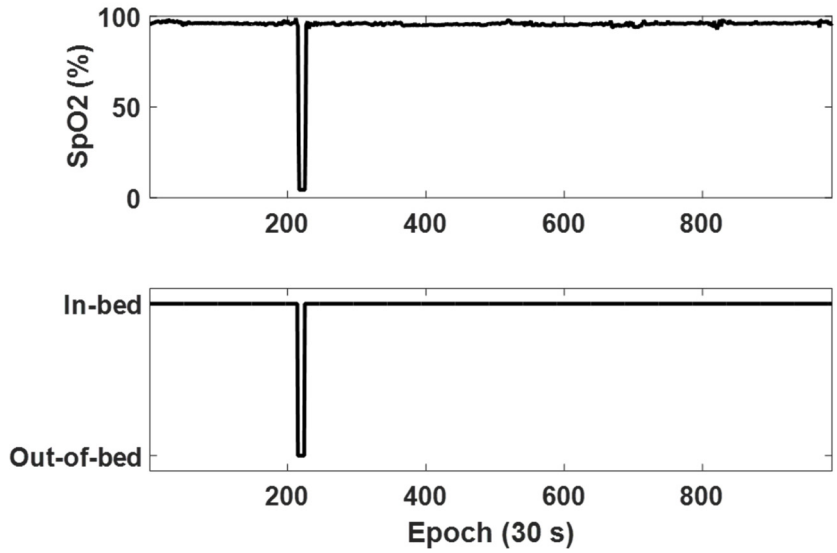

Figure 4-6. Correlation between estimated out of bed period and SpO2 during PSG.

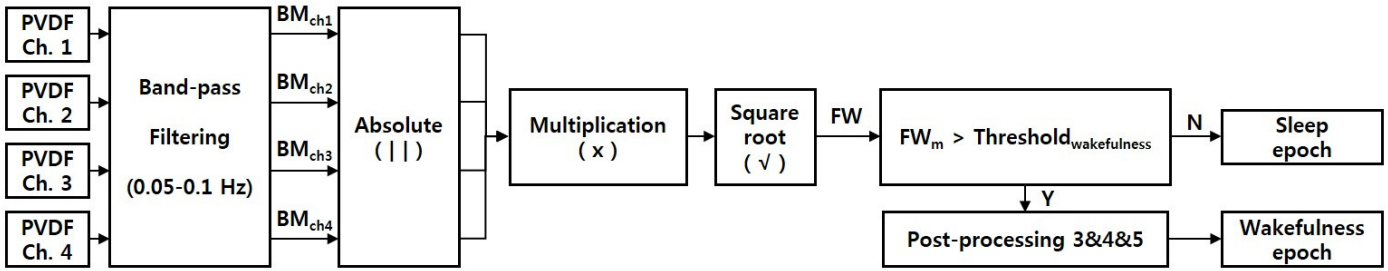

Figure 4-7. Wakefulness detection procedure.

4.1.4. SWS Detection

Figure 4-8 shows the average respiratory rate and hypnogram during PSG from the OSA patient #4. In this figure, the gray dashed squares indicate SWS periods. As shown in the figure, the variability of the respiratory rate during SWS (stage N3) is relatively stable compared with those of the other stages. On the basis of this phenomenon, the variability of the respiratory rate from the PVDF data was chosen as a feature for the SWS detection method.

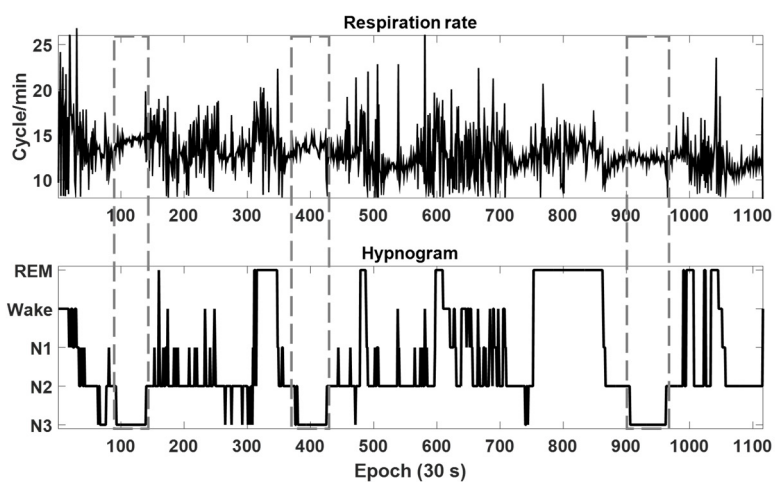

Figure 4-8. Average respiratory rate and hypnogram during PSG.

First, the average respiratory rate of each epoch (r_{rate}) was obtained using the same method as used to detect REM sleep. After the respiratory rate was obtained, the differences between adjacent elements of r_{rate} were calculated, and then these values were then squared. The feature used for the SWS detection from the respiratory rate (f_{rate}) can be described by the following equation:

$$\boldsymbol{f_{rate}[n] = \{r_{rate}[n] - r_{rate}[n-1]\}^2} \quad \textbf{(4-8)}$$

where $r_{rate}[n]$ denotes the respiratory rate of the *n*th epoch. After the feature extraction, the smoothed signal (s_{rate}) of f_{rate} was obtained by using the moving average filter with 10 epochs (300 s). In equation form, this is written as follows:

$$\boldsymbol{S_{rate}[n] = \frac{1}{M}\sum_{k=0}^{M-1} f_{rate}\,[n+k]} \quad \textbf{(4-9)}$$

where M is the number of points in the average. Examples of r_{rate}, f_{rate}, and s_{rate} from the OSA patient #4 are shown in Figure 4-9.

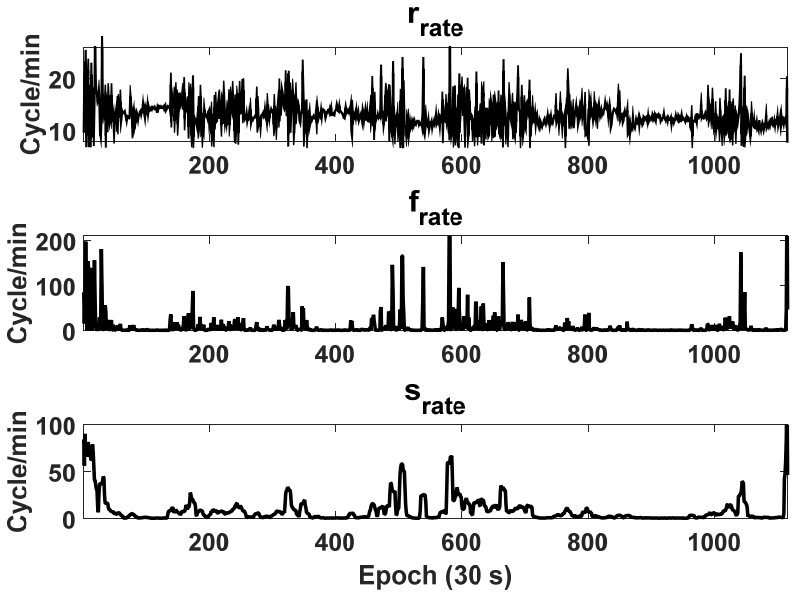

Figure 4-9. Respiratory rate, feature from respiratory rate, and smoothed feature

For the SWS detection, s_{rate} was compared with the threshold for SWS, which is described by the following equations:

$$\mathbf{M} = \frac{1}{N}\sum_{n=1}^{N} \boldsymbol{s_{rate}(n)} \quad \textbf{(4-10)}$$

$$\mathbf{k(n)} = \begin{cases} \mathbf{1}, & \boldsymbol{s_{rate} < M} \\ \mathbf{0}, & \boldsymbol{s_{rate} \geq M} \end{cases} \quad \textbf{(4-11)}$$

$$\mathbf{L} = \frac{1}{N}\sum_{n=1}^{N} \{\boldsymbol{s_{rate}(n) \cdot k(n)}\} \quad \textbf{(4-12)}$$

$$\boldsymbol{Threshold_{SWS} = L/5} \quad \textbf{(4-13)}$$

The *n*th epoch was determined as SWS if s_{rate} was less than $threshold_{sws}$; otherwise, it was non-SWS. The value used for $threshold_{sws}$ was based on the training dataset.

As shown in Figure 4-10, when the value for the threshold of the SWS detection was five, the mean performance was the highest. In this analysis, Cohen's kappa (k) coefficient was marked as the "mean performance". The final SWS epoch was determined through the post-processing.

Post-processing 6:

Estimated SWS sleep periods shorter than 10 min were rejected.

All of the SWS detection procedures are shown schematically in Figure 4-11. Figure 4-12 shows conceptual diagram of hierarchical classification of sleep stages.

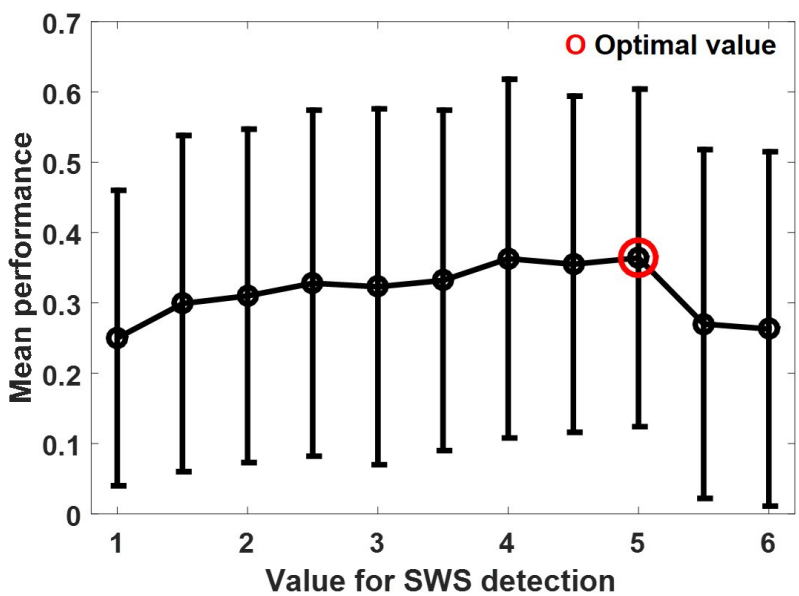

Figure 4-10. Value determination for threshold of SWS detection.

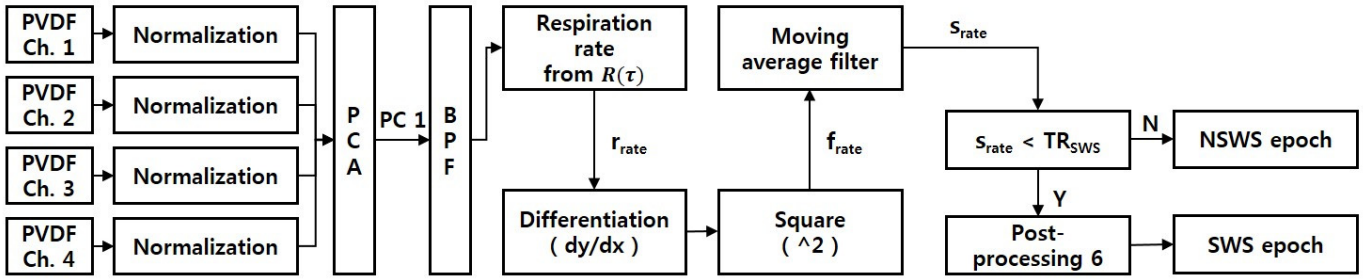

Figure 4-11. SWS detection procedure.

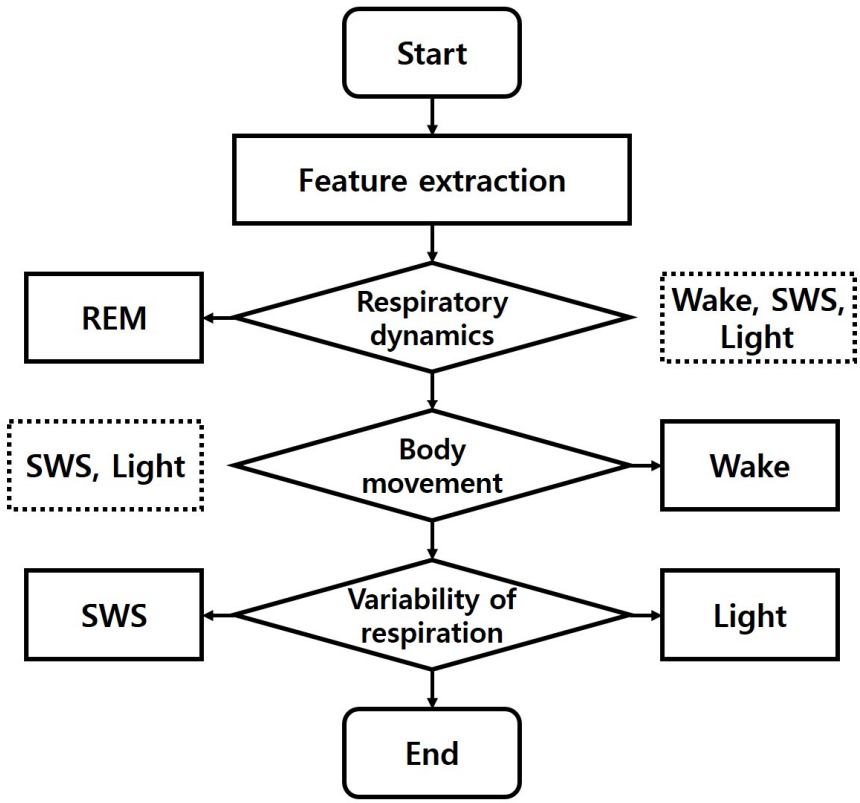

Figure 4-12. Diagram of hierarchical classification of sleep stages.

4.2. Results

4.2.1. REM Sleep Detection

The statistical results of the epoch-by-epoch REM sleep detection from the test dataset are listed in Table 4-3. In the results, sensitivity represents the proportion of correctly estimated REM sleep epochs, whereas specificity represents the proportion of correctly estimated NREM sleep epochs. From the Mann-Whitney-Wilcoxon test, no significant differences were observed in the sensitivity ($p = 0.98$), specificity ($p = 0.67$), accuracy ($p = 0.58$), and kappa values ($p = 0.96$) among the groups. The kappa statistical analysis revealed a substantial agreement ($0.6 < k < 0.8$) between the proposed method and the PSG for the normal, OSA, and the whole group. Figure 4-13 shows the durations of REM sleep from the proposed method and PSG. Based on the independent sample t-test, there was no significant difference in the REM sleep times between these two methods. Table 4-4 lists the results of a comparison of the REM sleep detection results from the proposed method and those from previous studies. As shown in the table, the proposed method has the highest REM sleep detection accuracy.

Table 4-3. Epoch-by-epoch REM sleep detection.

Set	Group	N	Sensitivity (%)	Specificity (%)	Accuracy (%)	Kappa
Training	Total	5	76.6±18.2	93.8±3.6	91.2±3.3	0.62±0.13
Test	Total	19	66.7±15.4	94.1±4.1	89.5±4.8	0.61±0.13
	Normal	9	67.3±15.6	94.6±4.2	90.4±4.5	0.62±0.13
	OSA	10	66.2±16.0	93.7±4.3	88.8±5.2	0.61±0.15

N: number of participants; OSA: obstructive sleep apnea

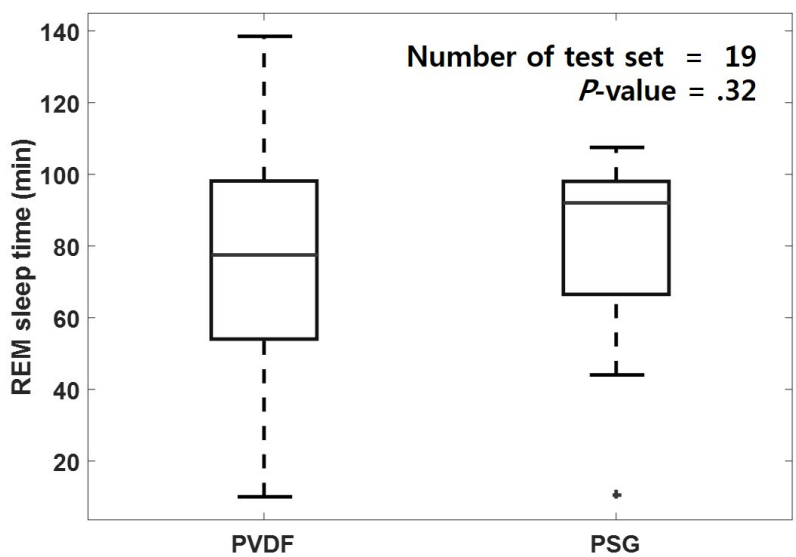

Figure 4-13. Durations of REM sleep from PSG and proposed method.

Table 4-4. Comparisons of REM sleep detection results with previous studies.

Author (year)	Signal	Sensor	N (Normal/OSA)	Accuracy (%)
Watanabe (2004)	Movement, BCG	Pneumatic	12 (12/0)	38.3 ± 20.3
Xiao (2013)	ECG	Ag/AgCl	45 (45/0)	59.8 ± 19.9
Kortelainen (2010)	BCG	EMFIT	18 (18/0)	80.0 ± 9.0
Tanida (2013)	ECG	Ag/AgCl	10 (10/0)	80.3 ± 4.2
Chung (2009)	Respiration	Thermocouple	22 (13/9)	87.7 ± 4.9
Chung (2009)	Respiration	Belt type	22 (13/9)	88.1 ± 5.0
Hwang (2015)	**Respiration**	**PVDF**	**19 (9/10)**	**89.5± 4.8**

OSA: obstructive sleep apnea; BCG: ballistocardiogram; ECG: electrocardiogram; EMFIT: electromechanical film; PVDF: polyvinylidene fluoride

4.2.2. Wakefulness Detection

The epoch-by-epoch results of the wakefulness detection are listed in Table 4-5. A kappa statistical analysis revealed a moderate agreement ($0.4 < k < 0.6$) between the proposed method and PSG for each training and test set. For the test set with more than 80% sleep efficiency, the average sensitivity of the wakefulness detection increased from 54.5% to 59.3%. Figure 4-14 shows the wakefulness detection results for the best case from the OSA patient #12. In this case, the sensitivity, specificity, accuracy, and kappa statistic were 68.0%, 96.9%, 93.3%, and 0.68, respectively. In this figure, the sleep/wake patterns from the PSG recording are shown for reference.

Table 4-5. Epoch-by-epoch wakefulness detection.

Set	N	Sensitivity (%)	Specificity (%)	Accuracy (%)	Kappa
Training	5	64.4±22.1	93.2±4.6	85.7±7.0	0.46±0.17
Test	19	54.5±14.7	93.6±3.0	86.6±4.6	0.46±0.10
S.E. > 80%	12	59.3±15.0	93.0±3.4	89.0±3.3	0.46±0.09

N: number of participants; S.E.: sleep efficiency

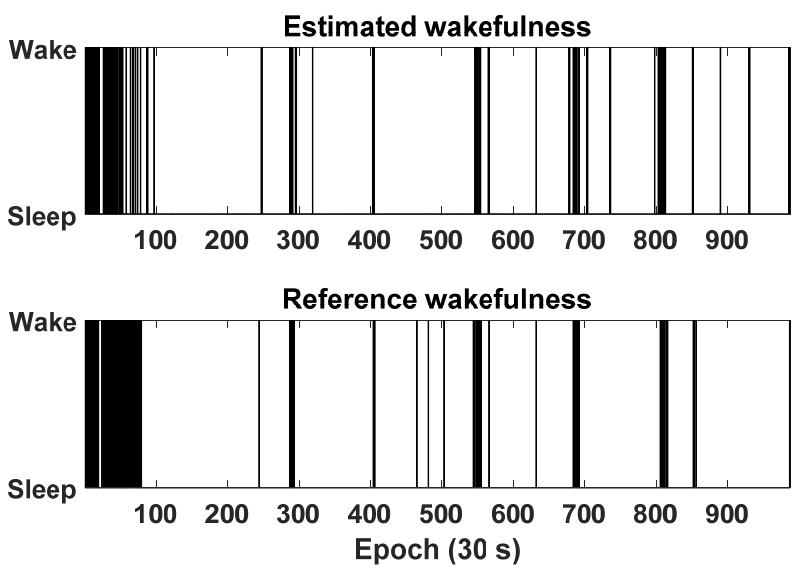

Figure 4-14. Epoch-by-epoch wakefulness detection results for best case.

The results from the proposed method are compared with those of other sleep/wake detection methods in Table 4-6. The results from an actigraphy based method [101] show a sensitivity similar to the proposed method. In other cases, the EMG based [102] and heart rate based methods [103] showed higher sensitivity and specificity than the PVDF based method. However, for EMG and heart rate recordings, the Ag/AgCl electrode must be attached to the body of the sleeper, and this can interrupt comfortable sleep.

Table 4-6. Comparisons of wakefulness detection results with previous studies.

Method	Actigraphy	AT EMG	Heart rate	**PVDF**
N	15	12	15	**19**
Sensitivity (%)	54.3	72.0	76.8	**54.5**
Specificity (%)	95.3	99.0	99.9	**93.6**
Accuracy (%)	90.7	79.0	n/a	**86.6**
Kappa	n/a	0.62	n/a	**0.46**

N: number of participants; AT EMG: anterior tibialis electromyography

4.2.3. SWS Detection

The epoch-by-epoch results of the SWS detection are listed in Table 4-7. The kappa statistical analysis revealed a fair agreement ($0.2 < k < 0.4$) between the proposed method and the PSG for each training and test set. However, 10 subjects had less than 40 epochs of SWS, and 6 subjects had less than 20 epochs of SWS in the test set. For the test set with over 20 SWS epochs, the average kappa value of the SWS detection increased from 0.33 to 0.41, and the corresponding value increased up to 0.48 for the test set with over 40 epochs. Figure 4-15 shows the SWS detection results for the best case from the OSA patient #4. In this case, the sensitivity, specificity, accuracy, and kappa statistic were 69.0%, 97.8%, 93.3%, and 0.72, respectively. In this figure, SWS/NSWS patterns from the PSG recording are shown for reference.

Table 4-7. Epoch-by-epoch SWS detection.

Set	N	Sensitivity (%)	Specificity (%)	Accuracy (%)	Kappa
Training	5	45.9±22.6	97.0±4.8	93.3±5.7	0.36±0.20
Test	19	40.7±25.6	96.5±3.2	92.4±5.2	0.33±0.26
SWS > 20 epochs	13	40.3±25.5	96.8±3.3	90.9±5.4	0.41±0.25
SWS > 40 epochs	9	44.8±20.1	97.2±3.7	89.7±6.0	0.48±0.20

N: number of participants; SWS: slow wave sleep

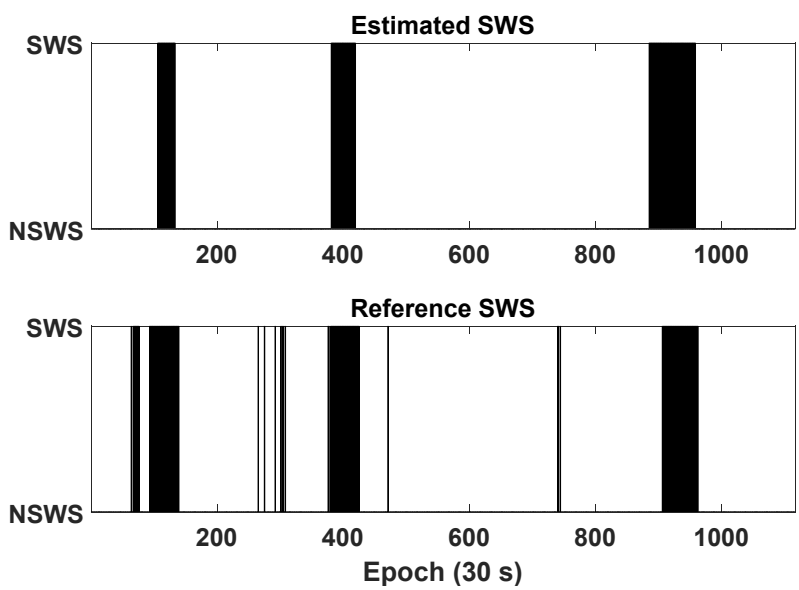

Figure 4-15. Epoch-by-epoch SWS detection results for best case.

4.2.4. Sleep Macro- and Microstructure Detection

The sleep stages of each subject were obtained from the REM sleep, wakefulness, and SWS detection results. For the estimated epoch, if the detection results overlapped, wakefulness had a higher priority than SWS, and REM sleep had a higher priority than wakefulness. Based on the PSG data scoring, the reference sleep stages were divided into four categories: SWS, light sleep, wakefulness, and REM sleep. Stages 1 and 2 were considered as light sleep. Stage 3 was considered as SWS. For the sleep macrostructure, the sleep stages were divided into three categories: NREM sleep, wakefulness, and REM sleep. Stages 1, 2, and 3 were considered as NREM sleep.

The epoch-by-epoch sleep stages detection results are listed in Table 4-8. From the Mann-Whitney-Wilcoxon test, no significant differences were observed in the accuracy ($p = 0.60$) and kappa values ($p = 0.84$) between the normal and OSA groups for the three stage classification. For the four stage classification, the corresponding values also showed no significant differences ($p = 0.13$, and $p = 0.18$) between the two groups. Table 4-9 presents a confusion matrix of all the subjects. The numbers in the table refer to the amounts of the corresponding epochs.

Table 4-8. Epoch-by-epoch sleep stages detection.

No. of stages	Set	Group	N	Accuracy (%)	Kappa
3	Training	Total	5	78.9±8.0	0.53±0.13
	Test	Total	19	78.6±5.7	0.54±0.12
		Normal	9	79.1±6.7	0.54±0.13
		OSA	10	78.1±4.9	0.53±0.11
4	Training	Total	5	72.9±8.1	0.48±0.10
	Test	Total	19	71.3±7.7	0.48±0.12
		Normal	9	68.6±9.7	0.46±0.15
		OSA	10	73.7±4.7	0.50±0.08

N: number of participants; OSA: obstructive sleep apnea

Table 4-9. Confusion matrix of all test dataset.

Overall		Estimation				
		SWS	Light	Wake	REM	Total
Reference	SWS	1139	842	66	5	2052
	Light	611	8643	748	436	10438
	Wake	70	1202	1436	176	2884
	REM	0	925	173	1748	2846
	Total	1820	11612	2423	2365	18220

SWS: slow wave sleep; REM: rapid eye movement

Table 4-10 lists the results of the comparison between the sleep stages detection results from the proposed method and those from previous methods. For the macrostructure (three stage) detection, the sleep stages detection performance of the ECG based methods [65, 68] was lower than that of the proposed method. In other studies [70-72], the EMFIT based methods showed a slightly higher accuracy than the proposed method, but the kappa value was lower than that of the PVDF based method [71]. For the microstructure (four stage) detection, the ECG based methods [66, 67] had lower accuracies and kappa values than the proposed method. The PAT based method [69] showed a similar kappa value compared with the proposed method, but the accuracy was lower than that of the proposed method.

Figure 4-16 shows the sleep stages detection results for the best case (Figure 4-16(a), OSA patient #1) and worst case (Figure 4-16(b), normal subject #11). In the best case, the accuracy and kappa statistics were 88.3% and 0.75, respectively. In the worst case, the corresponding values were 61.2% and 0.26, respectively.

Table 4-10. Comparisons of sleep stages detection results with previous studies.

No. of stages	Author (year)	N	Sensor	Signal	Accuracy (%)	Kappa
3 (Macro structure)	Watanabe (2004)	12	Air cushion	BCG, respiration, movement	42.8	n/a
	Redmond (2006)	37	Ag/AgCl	ECG	67.0	0.32
	Kortelaine (2010)	9	EMFIT	BCG, movement	79.0	0.44
	Xiao (2013)	45	Ag/AgCl	ECG	72.6	0.46
	Samy (2014)	7	Pressure sensitive bed	Respiration, movement	72.2	n/a
	Hwang (2015)	**19**	**PVDF**	**Respiration, movement**	**78.6**	**0.54**
4 (Micro structure)	Hender (2011)	227	Watch-PAT100	PAT, PPG, actigraphy	65.6	0.48
	Isa (2011)	16	Ag/AgCl	ECG	60.3	0.26
	Tanida (2013)	23	Ag/AgCl	ECG	56.0	n/a
	Hwang (2015)	**19**	**PVDF**	**Respiration, movement**	**71.6**	**0.48**

N: number of participants; EMFIT: electromechanical film; PVDF: polyvinylidene fluoride; BCG: ballistocardiogram; ECG: electrocardiogram; PAT: peripheral arterial tone; PPG: photoplethysmogram

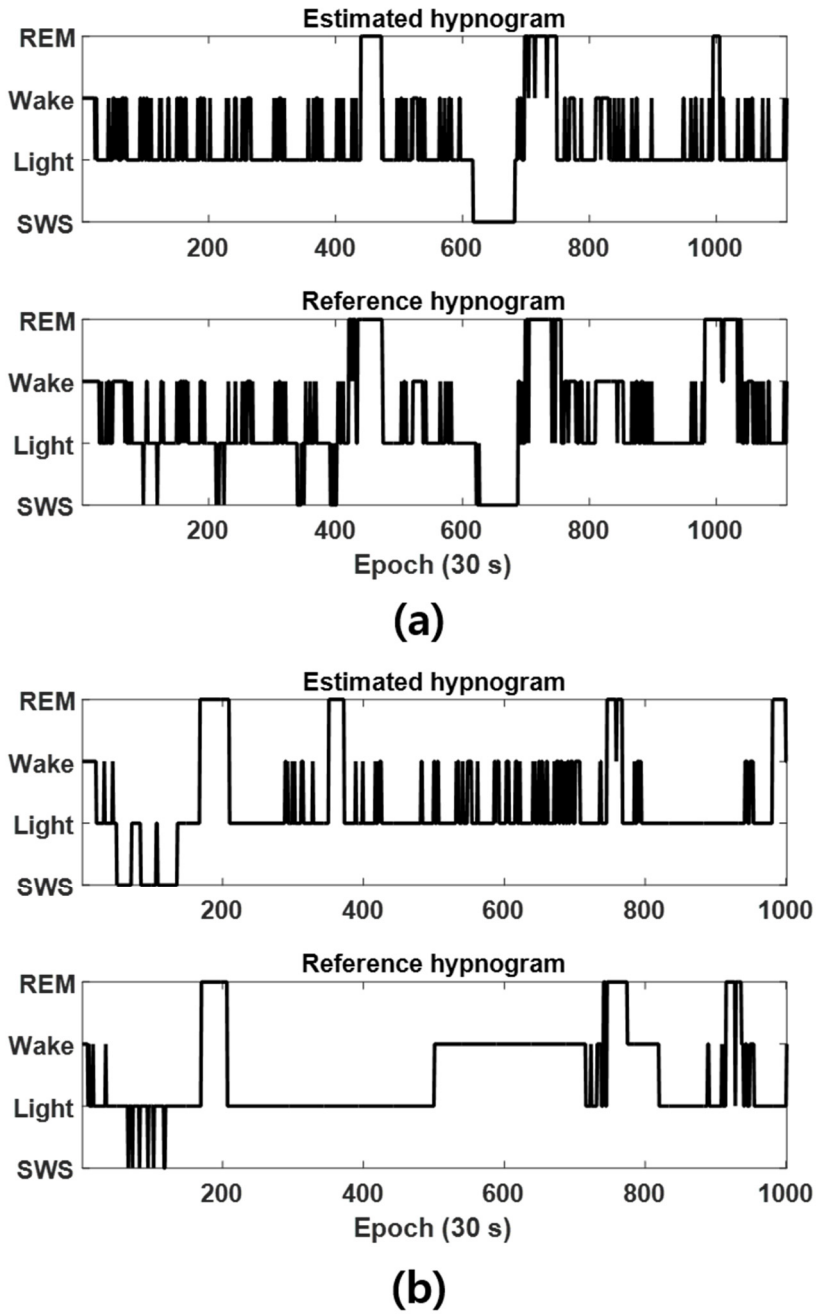

Figure 4-16. Sleep stages detection results for the best and worst cases.

4.3. Discussion

4.3.1. Agreement between Proposed Method and PSG

The sleep stages detection process was based on the following steps: 1) extraction of the respiratory rate and body movement signal from the PVDF data; 2) REM sleep detection from the dynamics of the respiratory signal; 3) wakefulness detection from the body movement signal; 4) SWS detection from the variability of the respiratory rate; and 5) sleep stages determination using the estimated REM sleep, wakefulness, and SWS epoch. To evaluate the algorithm, the proposed method was applied to the test dataset. In the epoch-by-epoch analysis (Table 4-8) for sleep macrostructure detection, the average value of the kappa statistics revealed greater than moderate agreement ($k > 0.4$), whereas the overall accuracy was 78.6%. For the sleep microstructure detection, the corresponding values were 0.48 and 71.3%, respectively. As listed in Table 4-8, no significant differences were observed in the sleep stages detection performance between the normal and OSA groups. This result demonstrated that the proposed sleep stages detection method is applicable not only to normal subjects but also to OSA patients.

4.3.2. Comparisons with Previous Studies

The proposed sleep stages detection method had a higher than or similar performance to previous ECG based methods or unconstrained sleep stages detection methods (Table 4-10). The ECG based sleep macrostructure detection methods showed the possibility of sleep stages detection based on HRV analysis [65, 68].

Even though these methods employed a constrained style using an Ag/AgCl electrode, no significant differences were observed in the sleep stages detection results between the ECG based and the proposed methods. In addition, the ECG based methods tended to use a larger number of features (25-27 features).

Sleep macrostructure detection methods via unconstrained techniques have also been proposed in previous studies. Watanabe *et al.* showed the possibility of sleep stages detection using noninvasive and unrestrained means [70]. They used a pneumatic bio measurement sensor to estimate the sleep stages, but their overall accuracy was only 42.8%. Kortelainen *et al.* used the signals acquired through a bed sensor, which was composed of multiple pressure sensitive EMFIT foil electrodes, for sleep staging [71]. Even though they used a computerized hidden Markov model classifier to detect the sleep macrostructure, they arrived at a kappa value of only 0.44, which was approximately 0.1 lower than the result obtained in this study. In addition, they only applied their system to healthy female subjects. Samy *et al.* proposed an unobtrusive method for sleep stages classification based on a high resolution pressure sensitive e-textile bed sheet [72]. In that study, the overall sleep stages detection accuracy was approximately 6% lower than the results in this study.

Sleep microstructure detection methods have also been proposed in the literature. In these studies, to the best of my knowledge, only constrained sensor based methods were applied. Isa *et al.* applied kernel dimensionality reduction to classify the sleep stages from an ECG signal [66]. They differentiated sleep into four stages (wake, light, REM, and SWS) based on the HRV features using a random forest classifier,

but the overall kappa value was only 0.26, which was approximately 0.2 lower than the result obtained by the proposed method. Tanida *et al.* compared a sleep analysis method based on power spectral indexes of the HRV data with PSG [67]. Even though they analyzed the sleep stages at a lower time resolution (minute-by-minute, the overall accuracy of the classification was 56.0%, whereas the method proposed in this study showed an overall accuracy of 71.3% for sleep microstructure detection. Hedner *et al.* proposed a sleep staging algorithm using signals derived from a portable monitoring device (Watch-PAT 100), which is based on PAT, pulse rate, and actigraphy [69]. Although they collected many physiological signals for sleep staging, its sleep stages detection accuracy was lower than the result obtained in this study. However, the number of analyzed datasets in this study was less than those of the PAT based study, and proposed sleep stages detection performance could be different when larger datasets are used.

In summary, the previous methods for the detection of the macrostructure or microstructure of sleep arrived at lower agreement results than this method. Even though the previous studies showed the possibility of sleep stages detection based on the use of a cardiorespiratory signal, sleep apnea or snoring detection methodologies were not provided in the mentioned studies, which may be a great novelty factor of the method proposed in this study.

4.3.3. Validation of Sleep Stages Detection Algorithm

As listed in Table 4-10, many of the sleep stages analysis studies categorized sleep into three stages: NREM sleep, REM sleep, and wakefulness. One could speculate that detecting SWS is relatively difficult compared with other sleep stages. Nevertheless, a sleep stages detection method that includes the SWS stage was established and tested in this study using PVDF data.

For the REM sleep detection, the respiratory rate of each subject was unconstrainedly obtained from the PVDF data, and REM sleep was estimated based on the respiratory related features. In OSA patients, the respiratory rate during sleep can be affected by the absence of breathing. Therefore, the REM detection results from the OSA patients were compared with those from normal subjects (Table 4-3). However, according to the result, no significant differences were observed in the sensitivity, specificity, accuracy, and kappa values between the groups. One could speculate that relatively long time based adaptive thresholds (7500 s, Table 4-2, which were unaffected by the changes in the instantaneous respiratory rate by the OSA occurrence, were appropriate for both normal subjects and OSA patients. Consequently, the proposed REM sleep detection method could accurately detect REM sleep without being affected by the severity of breathing disorders.

As mentioned earlier, thermocouple sensor based REM sleep detection method [98] was modified for the PVDF data. The thermocouple sensor used in a previous study was attached to the philtrum during an overnight PSG recording, and this could affect the normal sleep of a subject because of the inconvenience due to the direct electrode

attachment. In this study, sleep could be classified into "four stages," including REM sleep in an unconstrained manner, using the PVDF sensor, which is the main differentiating factor of this study from the previous one. Quantitatively, the REM sleep detection accuracy from the PVDF data (89.5%) showed similar performance compared with that from the nasal airflow signal (88.6%) for the same subjects. This result demonstrated that the proposed REM sleep detection method is applicable to respiratory signals from various sensors.

For the wakefulness detection, the threshold was set according to the PVDF data amplitude and variance. Therefore, an individual threshold could be applied to each subject. As listed in Table 4-5, the sensitivity of the wakefulness detection was lower than the specificity. When a subject was in a waking state without any movement, the proposed algorithm wrongly estimated the status because the wakefulness epoch was estimated based on the body movement signals from the PVDF data. This drawback of the movement based methods was also reported in the previous actigraph based methods [101, 104, 105], which reflected a trade-off between the sleep/wake detection performance and unconstrained monitoring. Therefore, the proposed method showed a performance similar to that of the previous actigraph based method [101].

For the SWS detection, the variability of the respiratory rate from the PVDF data was chosen as an indicator for the method. In short, a period during which the variability was relatively stable compared with the other periods was estimated as an SWS epoch. Regular and stable respiratory patterns in SWS have been reported in

the literature [106, 107]. As listed in Table 4-7, 10 of the 20 subjects had less than 20 min (40 epochs) of SWS. In these cases, the kappa values were considerably reduced despite a few wrong estimations only. Furthermore, two (OSA #7 and normal #6) among the test set subjects slept with no SWS epoch, and the kappa value was inevitably calculated to be zero in these cases. Actually, the kappa value remarkably increased up to 0.48 for the cases with SWS > 40 epochs. Despite these deficiencies, the overall SWS epoch detection accuracy was greater than 90%, whereas a previous sleep microstructure detection method revealed an accuracy of 80% for SWS classification from other sleep stages [67].

CHAPTER 5. CONCLUSION

PSG has been regarded as a standard method for the assessment of sleep; however, this method has a few limitations. To overcome these, many alternative sleep monitoring methods have been attempted to analyze sleep without PSG. However, most of these methods had limitations such that they could not unconstrainedly measure physiological signals, which made them unsuitable for daily sleep monitoring. Even though unconstrained sleep monitoring methods have also been proposed, they showed significantly lower sleep monitoring performance when compared with constrained sensor methods. Furthermore, integrated sleep monitoring methods that can simultaneously analyze both the sleep stages and SRBD events have rarely been studied.

In this study, new sleep stages and SRBD monitoring methods using a PVDF sensor were proposed. These methods can measure respiration, snoring, and body movement signals from subjects unconstrainedly. Using a single setup of this PVDF sensor, sleep apnea, snoring, and the sleep microstructure could be monitored simultaneously. The sleep apnea monitoring method revealed a high correlation coefficient ($r = 0.94$) between the AHI from PSG and the AHI from the proposed method. The snoring monitoring method classified snore events with 94.6% sensitivity and with 97.5% PPV. The sleep stage monitoring method showed that sleep can be divided into four stages from the PVDF data, with an average accuracy of over 70%. Experimental results demonstrated that the sleep stage and SRBD

detection performances were comparable to those of ambulatory devices and constrained sensor studies. Furthermore, the proposed method requires neither complex processing nor trained sleep experts. In conclusion, the developed system and methods could be applied to a sleep monitoring system in a residential or ambulatory environment.

REFERENCES

[1] L. Xie, H. Kang, Q. Xu, M. J. Chen, Y. Liao, M. Thiyagarajan, J. O'Donnell, D. J. Christensen, C. Nicholson, J. J. Iliff, T. Takano, R. Deane, and M. Nedergaard, Sleep drives metabolite clearance from the adult brain, Science, 342:373-7, 2013.

[2] E. Van Cauter, R. Leproult, and L. Plat, Age-related changes in slow wave sleep and REM sleep and relationship with growth hormone and cortisol levels in healthy men, J. A. Med. Assoc., 284:861-8, 2000.

[3] J. M. Siegel, Clues to the functions of mammalian sleep, Nature, 437:1264-71, 2005.

[4] M. Mirmiran, J. Scholtens, N. E. van de Poll, H. B. Uylings, J. van der Gugten, and G. J. Boer, Effects of experimental suppression of active (REM) sleep during early development upon adult brain and behavior in the rat, Brain Res., 283:277-86, 1983.

[5] G. A. Marks, J. P. Shaffery, A. Oksenberg, S. G. Speciale, and H. P. Roffwarg, A functional role for REM sleep in brain maturation, Behav. Brain Res., 69:1-11, 1995.

[6] M. J. Morrissey, S. P. Duntley, A. M. Anch, and R. Nonneman, Active sleep and its role in the prevention of apoptosis in the developing brain, Med. Hypotheses, 62:876-9, 2004.

[7] C. B. Saper, T. E. Scammell, and J. Lu, Hypothalamic regulation of sleep and circadian rhythms, Nature, 437:1257-63, 2005.

[8] R. Stickgold, Sleep-dependent memory consolidation, Nature, 437:1272-8, 2005.

[9] J. Born, B. Rasch, and S. Gais, Sleep to remember, Neuroscientist, 12:410-24, 2006.

[10] T. H. Turner, S. P. Drummond, J. S. Salamat, and G. G. Brown, Effects of 42 hr of total sleep deprivation on component processes of verbal working

memory, Neuropsychology, 21:787-95, 2007.

[11] M. W. Brown and J. P. Aggleton, Recognition memory: What are the roles of the perirhinal cortex and hippocampus?, Nat. Rev. Neurosci., 2:51-61, 2001.

[12] M. J. Fosse, R. Fosse, J. A. Hobson, and R. J. Stickgold, Dreaming and episodic memory: a functional dissociation?, J. Cogn. Neurosci., 15:1-9, 2003.

[13] D. F. Kripke, L. Garfinkel, D. L. Wingard, M. R. Klauber, and M. R. Marler, Mortality associated with sleep duration and insomnia, Arch. Gen. Psychiatry, 59:131-6, 2002.

[14] K. Spiegel, R. Leproult, and E. Van Cauter, Impact of sleep debt on metabolic and endocrine function, Lancet, 354:1435-9, 1999.

[15] F. P. Cappuccio, F. M. Taggart, N. B. Kandala, A. Currie, E. Peile, S. Stranges, and M. A. Miller, Meta-analysis of short sleep duration and obesity in children and adults, Sleep, 31:619-26, 2008.

[16] K. L. Knutson and E. Cauter, Associations between sleep loss and increased risk of obesity and diabetes, Ann. N. Y. Acad. Sci., 1129:287-304, 2008.

[17] N. Rogers, N. Price, J. Mullington, M. Szuba, H. Van Dongen, and D. Dinges, Plasma cortisol changes following chronic sleep restriction, Sleep, 23:A70-A71, 2000.

[18] R. Leproult and E. Van Cauter, Role of sleep and sleep loss in hormonal release and metabolism, Endocr. Dev., 17:11-21, 2010.

[19] M. Irwin, J. McClintick, C. Costlow, M. Fortner, J. White, and J. C. Gillin, Partial night sleep deprivation reduces natural killer and cellular immune responses in humans, FASEB J., 10:643-53, 1996.

[20] L. Redwine, R. L. Hauger, J. C. Gillin, and M. Irwin, Effects of sleep and sleep deprivation on interleukin-6, growth hormone, cortisol, and melatonin levels in humans, J. Clin. Endocrinol. Metab., 85:3597-603, 2000.

[21] K. Spiegel, J. F. Sheridan, and E. Van Cauter, Effect of sleep deprivation on response to immunization, J. A. Med. Assoc., 288:1471-2, 2002.

[22] Y. Liu, H. Tanaka, and G. Fukuoka Heart Study, Overtime work, insufficient sleep, and risk of non-fatal acute myocardial infarction in Japanese men, Occup. Environ. Med., 59:447-51, 2002.

[23] N. T. Ayas, D. P. White, J. E. Manson, M. J. Stampfer, F. E. Speizer, A. Malhotra, and F. B. Hu, A prospective study of sleep duration and coronary heart disease in women, Arch. Intern. Med., 163:205-9, 2003.

[24] C. A. Kushida, M. R. Littner, T. Morgenthaler, C. A. Alessi, D. Bailey, J. Coleman, Jr., L. Friedman, M. Hirshkowitz, S. Kapen, M. Kramer, T. Lee-Chiong, D. L. Loube, J. Owens, J. P. Pancer, and M. Wise, Practice parameters for the indications for polysomnography and related procedures: an update for 2005, Sleep, 28:499-521, 2005.

[25] M. A. Carskadon and W. C. Dement, Normal Human Sleep: An Overview in *Principles and practice of sleep medicine*. 5th ed. Philadelphia, PA: Saunders/Elsevier, 2011.

[26] R. L. Wilkins, R. L. Sheldon, and S. J. Krider, Clinical Assessment In Respiratory Care. London: Elsevier mosby, 2010.

[27] B. El-Ad and P. Lavie, Effect of sleep apnea on cognition and mood, Int. Rev. Psychiatry, 17:277-82, 2005.

[28] M. Hirshkowitz, I. Karacan, A. Gurakar, and R. L. Williams, Hypertension, erectile dysfunction, and occult sleep apnea, Sleep, 12:223-32, 1989.

[29] S. Yan-fang and W. Yu-ping, Sleep-disordered breathing: impact on functional outcome of ischemic stroke patients, Sleep Med., 10:717-9, 2009.

[30] R. S. Leung, Sleep-disordered breathing: autonomic mechanisms and arrhythmias, Prog. Cardiovasc. Dis., 51:324-38, 2009.

[31] H. E. Resnick, S. Redline, E. Shahar, A. Gilpin, A. Newman, R. Walter, G. A. Ewy, B. V. Howard, N. M. Punjabi, and S. Sleep Heart Health, Diabetes and sleep disturbances: findings from the Sleep Heart Health Study, Diabetes Care, 26:702-9, 2003.

[32] Y. Peker, J. Hedner, A. Johansson, and M. Bende, Reduced hospitalization with cardiovascular and pulmonary disease in obstructive sleep apnea

patients on nasal CPAP treatment, Sleep, 20:645-53, 1997.

[33] T. Young, M. Palta, J. Dempsey, J. Skatrud, S. Weber, and S. Badr, The Occurrence of Sleep-Disordered Breathing among Middle-Aged Adults, N. Engl. J. Med., 328:1230-5, 1993.

[34] J. Kim, K. In, J. Kim, S. You, K. Kang, J. Shim, S. Lee, J. Lee, S. Lee, C. Park, and C. Shin, Prevalence of sleep-disordered breathing in middle-aged Korean men and women, Am. J. Respir. Crit. Care Med., 170:1108-13, 2004.

[35] P. E. Peppard, T. Young, J. H. Barnet, M. Palta, E. W. Hagen, and K. M. Hla, Increased Prevalence of Sleep-Disordered Breathing in Adults, Am. J. Epidemiol., 177:1006-14, 2013.

[36] P. de Chazal, C. Heneghan, E. Sheridan, R. Reilly, P. Nolan, and M. O'Malley, Automated processing of the single-lead electrocardiogram for the detection of obstructive sleep apnoea, IEEE Trans. Biomed. Eng., 50:686-96, 2003.

[37] H. Nakano, T. Tanigawao, T. Furukawa, and S. Nishima, Automatic detection of sleep-disordered breathing from a single-channel airflow record, Eur. Respir. J., 29:728-36, 2007.

[38] F. Roche, J. M. Gaspoz, I. Court-Fortune, P. Minini, V. Pichot, D. Duverney, F. Costes, J. R. Lacour, and J. C. Barthelemy, Screening of obstructive sleep apnea syndrome by heart rate variability analysis, Circulation, 100:1411-5, 1999.

[39] M. O. Mendez, A. M. Bianchi, M. Matteucci, S. Cerutti, and T. Penzel, Sleep Apnea Screening by Autoregressive Models From a Single ECG Lead, IEEE Trans. Biomed. Eng., 56:2838-50, 2009.

[40] Y. G. Lim, K. H. Hong, K. K. Kim, J. H. Shin, S. M. Lee, G. S. Chung, H. J. Baek, D. U. Jeong, and K. S. Park, Monitoring physiological signals using nonintrusive sensors installed in daily life equipment, Biomed. Eng. Lett., 1:11-20, 2011.

[41] N. T. Ayas, S. Pittman, M. MacDonald, and D. P. White, Assessment of a wrist-worn device in the detection of obstructive sleep apnea, Sleep Med., 4:435-42, 2003.

[42] D. P. White, T. J. Gibb, J. M. Wall, and P. R. Westbrook, Assessment of accuracy and analysis time of a novel device to monitor sleep and breathing in the home, Sleep, 18:115-26, 1995.

[43] American Academy of Sleep Medicine., The International Classification Of Sleep Disorders : Diagnostic And Coding Manual. 2nd ed. Westchester, Ill.: American Academy of Sleep Medicine, 2005.

[44] S. Scott, K. Ah-See, H. Richardson, and J. A. Wilson, A comparison of physician and patient perception of the problems of habitual snoring, Clin. Otolaryngol., 28:18-21, 2003.

[45] P. G. Norton, E. V. Dunn, and J. S. J. Haight, Snoring in Adults - Some Epidemiologic Aspects, Can. Med. Assoc. J., 128:674-5, 1983.

[46] F. Dalmasso and R. Prota, Snoring: analysis, measurement, clinical implications and applications, Eur. Respir. J., 9:146-59, 1996.

[47] E. Lugaresi, F. Cirignotta, G. Coccagna, and C. Piana, Some epidemiological data on snoring and cardiocirculatory disturbances, Sleep, 3:221-4, 1980.

[48] D. J. Gottlieb, Q. Yao, S. Redline, T. Ali, M. W. Mahowald, and S. H. H. S. R. Grp, Does snoring predict sleepiness independently of apnea and hypopnea frequency?, Am. J. Respir. Crit. Care Med., 162:1512-7, 2000.

[49] E. O. Bixler, A. N. Vgontzas, H.-M. Lin, T. Ten Have, B. E. Leiby, A. Vela-Bueno, and A. Kales, Association of hypertension and sleep-disordered breathing, Arch. Intern. Med., 160:2289-95, 2000.

[50] E. Lugaresi, Snoring, Electroen. Clin. Neuro., 39:59-64, 1975.

[51] M. H. Kryger, T. Roth, and W. C. Dement, Principles And Practice Of Sleep Medicine. 5th ed. Philadelphia, PA: Saunders/Elsevier, 2011.

[52] V. Hoffstein, S. Mateika, and S. Nash, Comparing perceptions and measurements of snoring, Sleep, 19:783-9, 1996.

[53] R. Bhattacharjee, L. Kheirandish-Gozal, G. Pillar, and D. Gozal, Cardiovascular complications of obstructive sleep apnea syndrome: evidence from children, Prog. Cardiovasc. Dis., 51:416-33, 2009.

[54] C. Iber and American Academy of Sleep Medicine., The AASM Manual For The Scoring Of Sleep And Associated Events : Rules, Terminology And Technical Specifications. Westchester, IL: American Academy of Sleep Medicine, 2012.

[55] T. Emoto, U. R. Abeyratne, Y. Chen, I. Kawata, M. Akutagawa, and Y. Kinouchi, Artificial neural networks for breathing and snoring episode detection in sleep sounds, Physiol. Meas., 33:1675-89, 2012.

[56] A. Azarbarzin and Z. M. Moussavi, Automatic and unsupervised snore sound extraction from respiratory sound signals, IEEE Trans. Biomed. Eng., 58:1156-62, 2011.

[57] A. Yadollahi and Z. Moussavi, Automatic breath and snore sounds classification from tracheal and ambient sounds recordings, Med. Eng. Phys., 32:985-90, 2010.

[58] W. D. Duckitt, S. K. Tuomi, and T. R. Niesler, Automatic detection, segmentation and assessment of snoring from ambient acoustic data, Physiol. Meas., 27:1047-56, 2006.

[59] M. Cavusoglu, M. Kamasak, O. Erogul, T. Ciloglu, Y. Serinagaoglu, and T. Akcam, An efficient method for snore/nonsnore classification of sleep sounds, Physiol. Meas., 28:841-53, 2007.

[60] D. Pevernagie, R. M. Aarts, and M. De Meyer, The acoustics of snoring, Sleep Med. Rev., 14:131-44, 2010.

[61] J. H. Shin, Y. J. Chee, D. U. Jeong, and K. S. Park, Nonconstrained sleep monitoring system and algorithms using air-mattress with balancing tube method, IEEE Trans. Inf. Technol. Biomed., 14:147-56, 2010.

[62] H. K. Lee, J. Lee, H. J. Kim, J. Y. Ha, and K. J. Lee, Snoring detection using a piezo snoring sensor based on hidden Markov models, Physiol. Meas., 34:N41-N49, 2013.

[63] M. H. Silber, S. Ancoli-Israel, M. H. Bonnet, S. Chokroverty, M. M. Grigg-Damberger, M. Hirshkowitz, S. Kapen, S. A. Keenan, M. H. Kryger, T. Penzel, M. R. Pressman, and C. Iber, The visual scoring of sleep in adults, J.

Clin. Sleep Med., 3:121-31, 2007.

[64] C. A. Czeisler, E. Weitzman, M. C. Moore-Ede, J. C. Zimmerman, and R. S. Knauer, Human sleep: its duration and organization depend on its circadian phase, Science, 210:1264-7, 1980.

[65] S. J. Redmond and C. Heneghan, Cardiorespiratory-based sleep staging in subjects with obstructive sleep apnea, IEEE Trans. Biomed. Eng., 53:485-96, 2006.

[66] S. M. Isa, I. Wasito, and A. M. Arymurthy, Kernel dimensionality reduction on sleep stage classification using ECG signal, Int. J. Comput. Science Issues, 8:115-23, 2011.

[67] K. Tanida, M. Shibata, and M. M. Heitkemper, Sleep Stage Assessment Using Power Spectral Indices of Heart Rate Variability With a Simple Algorithm: Limitations Clarified From Preliminary Study, Biol. Res. Nurs., 15:264-72, 2013.

[68] M. Xiao, H. Yan, J. Z. Song, Y. Z. Yang, and X. L. Yang, Sleep stages classification based on heart rate variability and random forest, Biomed. Signal Proces., 8:624-33, 2013.

[69] J. Hedner, D. P. White, A. Malhotra, S. Herscovici, S. D. Pittman, D. Zou, L. Grote, and G. Pillar, Sleep staging based on autonomic signals: a multi-center validation study, J. Clin. Sleep Med., 7:301-6, 2011.

[70] T. Watanabe and K. Watanabe, Noncontact method for sleep stage estimation, IEEE Trans. Biomed. Eng., 51:1735-48, 2004.

[71] J. M. Kortelainen, M. O. Mendez, A. M. Bianchi, M. Matteucci, and S. Cerutti, Sleep Staging Based on Signals Acquired Through Bed Sensor, IEEE Trans. Inf. Technol. Biomed., 14:776-85, 2010.

[72] L. Samy, M. C. Huang, J. J. Liu, W. Y. Xu, and M. Sarrafzadeh, Unobtrusive Sleep Stage Identification Using a Pressure-Sensitive Bed Sheet, IEEE Sensors J., 14:2092-101, 2014.

[73] M. A. O'Reilly and K. Hynynen, A PVDF receiver for ultrasound monitoring of transcranial focused ultrasound therapy, IEEE Trans. Biomed. Eng.,

57:2286-94, 2010.

[74] S. H. Hwang, H. N. Yoon, D. W. Jung, Y. J. Lee, D. U. Jeong, and K. S. Park, "Apnea Event Estimation During Sleep Using Polyvinylidene Fluoride Film," in *eTELEMED 2013, The Fifth International Conference on eHealth, Telemedicine, and Social Medicine*, 2013, pp. 280-3.

[75] J. Siivola, New noninvasive piezoelectric transducer for recording of respiration, heart rate and body movements, Med. Biol. Eng. Comput., 27:423-5, 1989.

[76] S. J. Choi and Z. W. Jiang, A novel wearable sensor device with conductive fabric and PVDF film for monitoring cardiorespiratory signals, Sensor Actuat. A-Phys., 128:317-26, 2006.

[77] G. Roopa Manjunatha, K. Rajanna, D. R. Mahapatra, M. M. Nayak, U. M. Krishnaswamy, and R. Srinivasa, Polyvinylidene fluoride film based nasal sensor to monitor human respiration pattern: An initial clinical study, J. Clin. Monit. Comput., 27:647-57, 2013.

[78] F. Wang, M. Tanaka, and S. Chonan, Development of a PVDF piezopolymer sensor for unconstrained in-sleep cardiorespiratory monitoring, J. Intel. Mat. Syst. Str., 14:185-90, 2003.

[79] Y. Y. Chiu, W. Y. Lin, H. Y. Wang, S. B. Huang, and M. H. Wu, Development of a piezoelectric polyvinylidene fluoride (PVDF) polymer-based sensor patch for simultaneous heartbeat and respiration monitoring, Sensor Actuat. A-Phys., 189:328-34, 2013.

[80] H. J. Baek, G. S. Chung, K. K. Kim, and K. S. Park, A smart health monitoring chair for nonintrusive measurement of biological signals, IEEE Trans. Inf. Technol. Biomed., 16:150-8, 2012.

[81] R. B. Berry, G. L. Koch, S. Trautz, and M. H. Wagner, Comparison of respiratory event detection by a polyvinylidene fluoride film airflow sensor and a pneumotachograph in sleep apnea patients, Chest, 128:1331-8, 2005.

[82] B. B. Koo, C. Drummond, S. Surovec, N. Johnson, S. A. Marvin, and S. Redline, Validation of a polyvinylidene fluoride impedance sensor for

respiratory event classification during polysomnography, J. Clin. Sleep Med., 7:479-85, 2011.

[83] M. B. Norman, S. Middleton, O. Erskine, P. G. Middleton, J. R. Wheatley, and C. E. Sullivan, Validation of the Sonomat: a contactless monitoring system used for the diagnosis of sleep disordered breathing, Sleep, 37:1477-87, 2014.

[84] S. H. Hwang, C. M. Han, H. N. Yoon, D. W. Jung, Y. J. Lee, D. U. Jeong, and K. S. Park, Polyvinylidene fluoride sensor-based method for unconstrained snoring detection, Physiol. Meas., 36:1399-414, 2015.

[85] S. H. Hwang, H. J. Lee, H. N. Yoon, D. W. Jung, Y. J. G. Lee, Y. J. Lee, D. U. Jeong, and K. S. Park, Unconstrained Sleep Apnea Monitoring Using Polyvinylidene Fluoride Film-Based Sensor, IEEE Trans. Biomed. Eng., 61:2125-34, 2014.

[86] R. O. Duda, P. E. Hart, and D. G. Stork, Pattern Classification. 2nd ed. New York: Wiley, 2001.

[87] J. M. Bland and D. G. Altman, Statistical Methods for Assessing Agreement between Two Methods of Clinical Measurement, Lancet, 1:307-10, 1986.

[88] A. J. Viera and J. M. Garrett, Understanding interobserver agreement: the kappa statistic, Fam. Med., 37:360-3, 2005.

[89] J. H. Han, H. B. Shin, D. U. Jeong, and K. S. Park, Detection of apneic events from single channel nasal airflow using 2nd derivative method, Comput. Meth. Prog. Bio., 91:199-207, 2008.

[90] J. R. Landis and G. G. Koch, The measurement of observer agreement for categorical data, Biometrics, 33:159-74, 1977.

[91] R. P. Schnall, A. Shlitner, J. Sheffy, R. Kedar, and P. Lavie, Periodic, profound peripheral vasoconstriction - A new marker of obstructive sleep apnea, Sleep, 22:939-46, 1999.

[92] C. Cortes and V. Vapnik, Support-Vector Networks, Mach. Learn., 20:273-97, 1995.

[93] A. Aizerman, E. M. Braverman, and L. Rozoner, Theoretical foundations of

the potential function method in pattern recognition learning, Autom. Remote Control, 25:821-37, 1964.

[94] W. H. Kruskal and W. A. Wallis, Use of Ranks in One-Criterion Variance Analysis, J. Am. Statist. Assoc., 47:583-621, 1952.

[95] C. W. Hsu and C. J. Lin, A comparison of methods for multiclass support vector machines, IEEE Trans. Neural Netw., 13:415-25, 2002.

[96] L. M. Manevitz and M. Yousef, One-class SVMs for document classification, J. Mach. Learn. Res., 2:139-54, 2002.

[97] A. Oksenberg and D. S. Silverberg, The effect of body posture on sleep-related breathing disorders: facts and therapeutic implications, Sleep Med. Rev., 2:139-62, 1998.

[98] G. S. Chung, B. H. Choi, J. S. Lee, J. S. Lee, D. U. Jeong, and K. S. Park, REM sleep estimation only using respiratory dynamics, Physiol. Meas., 30:1327-40, 2009.

[99] S. H. Hwang, H. N. Yoon, D. W. Jung, S. W. Seo, Y. J. Lee, D. U. Jeong, and K. S. Park, Unconstrained REM Sleep Monitoring Using Polyvinylidene Fluoride Film-Based Sensor in the Normal and the Obstructive Sleep Apnea Patients, J. Biomed. Eng. Res., 35:55-61, 2014.

[100] W. S. Cleveland, Robust Locally Weighted Regression and Smoothing Scatterplots, J. Am. Statist. Assoc., 74:829-36, 1979.

[101] J. Paquet, A. Kawinska, and J. Carrier, Wake detection capacity of actigraphy during sleep, Sleep, 30:1362-9, 2007.

[102] S. H. Hwang, G. S. Chung, J. S. Lee, J. H. Shin, S. J. Lee, D. U. Jeong, and K. Park, Sleep/wake estimation using only anterior tibialis electromyography data, Biomed. Eng. Online, 11:1-15, 2012.

[103] A. Bulckaert, V. Exadaktylos, G. De Bruyne, B. Haex, E. De Valck, J. Wuyts, J. Verbraecken, and D. Berckmans, Heart rate-based nighttime awakening detection, Eur. J. Appl. Physiol., 109:317-22, 2010.

[104] L. de Souza, A. A. Benedito-Silva, M. L. N. Pires, D. Poyares, S. Tufik, and H. M. Calil, Further validation of actigraphy for sleep studies, Sleep, 26:81-

5, 2003.

[105] D. F. Kripke, D. J. Mullaney, S. Messin, and V. G. Wyborney, Wrist Actigraphic Measures of Sleep and Rhythms, Electroen. Clin. Neuro., 44:674-6, 1978.

[106] N. J. Douglas, D. P. White, C. K. Pickett, J. V. Weil, and C. W. Zwillich, Respiration during sleep in normal man, Thorax, 37:840-4, 1982.

[107] E. A. Phillipson, Control of breathing during sleep, Am. Rev. Respir. Dis., 118:909-39, 1978.

국문 초록

PVDF 필름 센서를 사용한 수면관련 호흡장애 및 수면 단계의 무구속적 모니터링

이 연구에서는 PVDF 필름 센서를 사용하여 무구속적으로 수면관련 호흡장애 및 수면 단계를 모니터링 할 수 있는 기법을 개발하였다. PVDF 센서는 4 x 1 배열로 구성되었으며, 센서 시스템의 총 두께는 약 1.1mm 였다. PVDF 센서는 침대보와 매트리스 사이에 위치시켜 참가자의 몸에 직접적인 접촉이 없도록 하였다.

수면무호흡증 검출 연구에는 26 명의 수면무호흡증 환자와 6 명의 정상인이 참가하였다. PVDF 신호의 표준편차에 근거하여 수면무호흡증 검출 방법을 개발하였고, 추정된 수면무호흡증 검출 결과를 수면 전문의의 판독 결과와 비교하였다. 추정된 결과와 판독 결과 간의 수면 무호흡-저호흡 지수 상관계수는 $0.94\ (p < 0.001)$ 이었다.

코골이 검출 연구에는 총 20 명의 수면무호흡증 환자가 참가하였다. PVDF 신호를 단시간 푸리에 변환하여 얻은 파워 비율과 최대 주파수를 주파수 영역 특징으로 추출하였다. 추출된 특징들을 서포트 벡터 머신 분류기에 입력하였고, 분류기의 검출 결과에 따라 코골이 또는 코골이가

아닌 구간으로 나누었다. 제안된 방법에서 추정한 코골이 검출 결과를 정상 성인 3 명의 청각 및 시각 기반 코골이 판독 결과와 비교하였다. 코골이 검출에 대한 평균 민감도 및 양성예측도는 각각 94.6% 및 97.5% 이었다.

수면 단계 검출 연구에는 11 명의 정상인과 13 명의 수면무호흡증 환자가 참가하였다. 렘 (REM) 수면 구간은 호흡의 주기와 그 변동률에 근거하여 추정하였다. 깸 구간은 움직임 신호에 근거하여 추정하였다. 깊은 수면 구간은 분당 호흡수의 변화폭에 기반하여 추정하였다. 각 수면 단계 검출 결과를 통합하여 최종 결과를 수면 전문의의 판독 결과와 비교하였다. 30 초 단위로 수면 단계를 검출하였을 때, 평균 정확도는 71.3% 이었으며 평균 카파 값은 0.48 이었다.

연구에서 제안된 PVDF 센서와 알고리즘을 통하여 상용화된 수면 모니터링 장치에 비교할 수 있을 만한 수준의 성능을 확보하였다. 이 연구 결과가 가정환경 기반 수면모니터링 시스템의 활용도와 정확도를 높이는데 기여할 수 있을 것으로 기대한다.

주요어 : 무구속 계측, 수면 무호흡증, 코골이, 수면 단계, PVDF 센서

학 번 : 2009-23196